Supplementary material: Enhanced low-frequency vibration energy harvesting with inertial amplifiers

Sondipon Adhikari[1,*] **and Arnab Banerjee**[2]

[1]College of Engineering, Swansea University, Swansea, UK
[2]Department of Civil Engineering, Indian Institute of Technology Delhi, India
[*]s.adhikari@swansea.ac.uk

ABSTRACT

Piezoelectric vibration energy harvesters have demonstrated the potential for sustainable energy generation from diverse ambient sources in the context of low-powered micro-scale systems. However, challenges remain concerning harvesting more power from low-frequency input excitations and broadband random excitations. To address this, here we propose a purely mechanical approach by employing inertial amplifiers with cantilever piezoelectric vibration energy harvesters. The proposed mechanism can achieve inertial amplification amounting to orders of magnitude under certain conditions. Harmonic, as well as broadband random excitations, are considered. Two types of harvesting circuits, namely, without and with an inductor, have been employed. We explicitly demonstrate how different parameters describing the inertial amplifiers should be optimally tuned to maximise harvested power under different types of excitations and circuit configurations. It is possible to harvest 5 times more power at a 50% lower frequency when the ambient excitation is harmonic. Under random broadband ambient excitations, it is possible to harvest 10 times more power with optimally selected parameters.

1 Introduction

Vibration energy harvesting exploiting piezoelectric effect has been a growing research field over the past decade. The predicted rise of Internet of Things (IoT) and wireless sensor network for the development of digital twins of complex engineering systems will led to further interest in the vibration energy harvesting technology. A key challenge which hinders this growth is the inefficiency towards harvesting more power when the ambient vibration is low frequency and imprecisely known (random and broadband). This paper proposes a solution to address these two issues by employing a mechanical approach involving inertial amplifiers. This enhances the inertia without increasing the static mass of the harvester. Inertial amplifiers have been theoretically investigated to manipulate bandgaps in mechanical metamaterials. We bought this concept to vibration energy harvesting for the first time. Our results explicitly demonstrate increasing harvested power at significantly lower frequencies which is not possible without employing inertial amplifiers. The work is based on rigorous mathematical modelling from physics-based principles and analytical solutions of resulting differential equations. We also report an in-depth optimisation approach to derive the system parameters which maximise harvested power in different physically realistic situations. The pathways to impact will arise from the physical insights originating from closed-form results quantifying harvested power, general nondimensional nature of the analytical results, and formulae governing practical design of inertial amplifier enhanced energy harvesters. The proposed inertial amplifier will play a pivotal role in low-frequency lightweight energy harvesting.

We illustrate the background, expand mathematical methods and provide new data in support of the results and concepts presented in the main paper. This document contains additional results and new discussions which have not been presented in the main paper. The Supplementary material is organised as below.

Contents

2 Electromechanical model for cantilever piezoelectric energy harvesters

2.1 Equation of motion for piezoelectric cantilevers

Illustrative diagram of a cantilever vibration energy harvester with a bimorph piezoelectric patch is shown in Figure 1. Due to the small thickness to length ratio, Euler-Bernoulli beam theory is generally used to model bending vibration of such cantilevers [1]. The equation of motion of free-vibration of a damped cantilever modelled (see for example [2]) using Euler-Bernoulli beam theory can be expressed as

$$EI\frac{\partial^4 U(x,t)}{\partial x^4}+\rho_h A\frac{\partial^2 U(x,t)}{\partial t^2}+\widehat{c}_1\frac{\partial^5 U(x,t)}{\partial x^4\partial t}+\widehat{c}_2\frac{\partial U(x,t)}{\partial t}=0 \tag{1}$$

In the above equation x is the coordinate along the length of the beam, t is the time, E is the Young's modulus, I is the second-moment of the cross-section, A is the cross-section area, ρ_h is the density of the material and $U(x,t)$ is the transverse displacement. The length of the beam is assumed to be L. Additionally $\widehat{c}_1$ is the strain-rate-dependent damping coefficient, $\widehat{c}_2$ is the velocity-dependent viscous damping coefficient. The strain-rate-dependent damping can be used to model inherent damping property of the material of the cantilever beam. The velocity-dependent viscous damping can be used to model damping due to external factors.

The undamped natural frequencies (Hz) of the cantilever beam in (1) can be expressed as

$$f_j=\frac{\lambda_j^2}{2\pi}\sqrt{\frac{EI}{\rho_h AL^4}},\quad j=1,2,3,\cdots \tag{2}$$

where λ_j needs to be obtained by [3] solving the following transcendental equation

$$\cos\lambda\cosh\lambda+1=0 \tag{3}$$

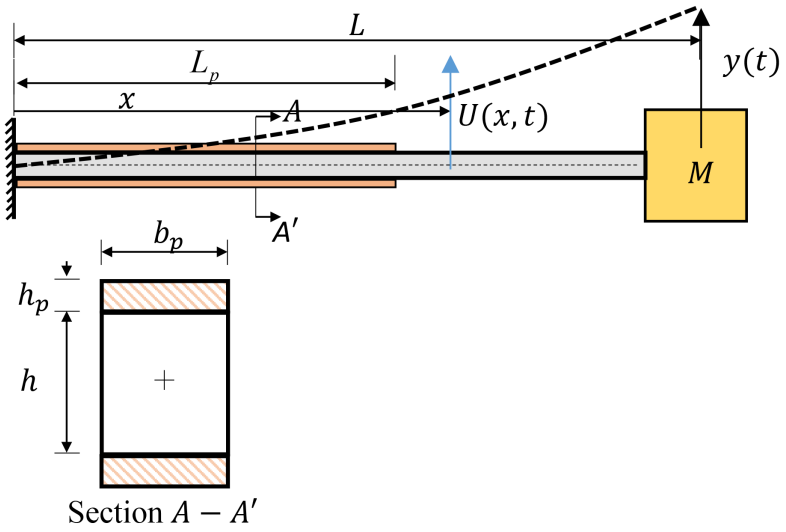

Figure 1. Cantilever piezoelectric energy harvesters in a bimorph configuration. The length of the cantilever is L and the length of the piezoelectric patch is L_p. The thickness of the beam is h and the thickness of the piezoelectric patch is h_p. The width of both the beam and the piezoelectric patch is b_p. The coordinate x is along the length of the beam originating at the fixed end. M is the tip mass fixed at the free end of the beam. The (continuous) displacement of the beam is given by $U(x,t)$ and the displacement of the tip mass is given by $y(t)$.

Solving this equation, the values of λ_j can be obtained as 1.8751, 4.69409, 7.8539 and 10.99557. For larger values of j, in general we have $\lambda_j = (2j-1)\pi/2$. The vibration mode shape corresponding to the j-th natural frequency can be expressed as

$$\psi_j(\xi) = (\cosh\lambda_j\xi - \cos\lambda_j\xi) - \left(\frac{\sinh\lambda_j - \sin\lambda_j}{\cosh\lambda_j + \cos\lambda_j}\right)(\sinh\lambda_j\xi - \sin\lambda_j\xi) \tag{4}$$

where

$$\xi = \frac{x}{L} \tag{5}$$

is the normalised coordinate along the length of the cantilever. For sensing applications we are primarily interested in the first few modes of vibration only.

Consider the mass M at the end of the cantilevered resonator in Figure 1. The boundary conditions with an additional mass of M at $x = L$ can be expressed as

$$U(0,t) = 0, \quad Z'(0,t) = 0, \quad Z''(L,t) = 0, \quad \text{and} \quad EIZ'''(L,t) - M\ddot{Z}(L,t) = 0 \tag{6}$$

Here $(\bullet)'$ denotes derivative with respective to x and $\dot{(\bullet)}$ denotes derivative with respective to t. It can be shown that (see for example [4]) the resonant frequencies are still obtained from equation (2) but λ_j should be obtained by solving

$$(\cos\lambda\sinh\lambda - \sin\lambda\cosh\lambda)\Delta M\lambda + (\cos\lambda\cosh\lambda + 1) = 0 \tag{7}$$

Here

$$\Delta M = \frac{M}{\rho_h AL} \tag{8}$$

is the ratio of the tip mass and the mass of the cantilever. If the tip mass is zero, then one can see that equation (8) reduces to equation (3).

2.2 Equivalent single-degree-of-freedom model

The equation of motion of the beam in (1) is a partial differential equation. This equation represents infinite number of degrees of freedom. The mathematical theory of linear partial differential equations is very well developed and the nature of solutions of the bending vibration is well understood. Considering a steady-state harmonic motion with frequency ω we have

$$U(x,t) = u(x)\exp[\mathrm{i}\omega t] \tag{9}$$

where $\mathrm{i} = \sqrt{-1}$. Substituting this in the beam equation (1) we have

$$EI\frac{\mathrm{d}^4u(x)}{\mathrm{d}x^4} + \mathrm{i}\omega\widehat{c_1}\frac{\mathrm{d}^4u(x)}{\mathrm{d}x^4} - \rho_h A\omega^2 u(x) + \mathrm{i}\omega\widehat{c_2}u(x) = 0 \tag{10}$$

Following the damping convention in dynamic analysis as in [5], we consider stiffness and mass proportional damping. Therefore, we express the damping constants as

$$\widehat{c_1} = \alpha_c(EI) \quad \text{and} \quad \widehat{c_2} = \beta_c(\rho A) \tag{11}$$

where α_c and β_c are stiffness and mass proportional damping factors.

Substituting these, from equation (10) we have

$$EI\frac{\mathrm{d}^4u(x)}{\mathrm{d}x^4} + \mathrm{i}\omega\left(\alpha_c EI\frac{\mathrm{d}^4u(x)}{\mathrm{d}x^4} + \beta_c\rho_h A u(x)\right) - \rho_h A\omega^2 u(x) = 0 \tag{12}$$

The first part of the damping expression is proportional to the stiffness term while the second part of the damping expression is proportional to the mass term. The general solution of equation (12) can be expressed as a linear superposition of all the vibration mode shapes (see for example [5]). Vibration energy harvesters are often designed to operate within a frequency range which is close to first few natural frequencies only. Therefore, without any loss of accuracy, simplified lumped parameter models can be used to corresponding correct resonant behaviour. This can be achieved using energy methods or more generally using Galerkin approach.

Assuming a unimodal solution, the dynamic response of the beam can be expressed as

$$U(x,t) = z_j(t)\psi_j(x), \quad j = 1,2,3,\cdots \tag{13}$$

Substituting this assumed motion into the equation of motion (1), multiplying by $\psi_j(x)$ and integrating by parts over the length one has

$$EIz_j(t)\int_0^L \psi_j''^2(x)\mathrm{d}x + \alpha_c EI\dot{z}_j(t)\int_0^L \psi_j''^2(x)\mathrm{d}x + \beta_c\rho_h A\dot{z}_j(t)\int_0^L \psi_j^2(x)\mathrm{d}x + \rho_h A\ddot{z}_j(t)\int_0^L \psi_j^2(x)\mathrm{d}x = 0 \tag{14}$$

Using the equivalent mass, damping and stiffness, this equation can be rewritten as

$$m_{eq_j}\ddot{z}_j(t) + c_{eq_j}\dot{z}_j(t) + k_{eq_j}z_j(t) = 0 \tag{15}$$

where the equivalent mass and stiffness terms are given by

$$m_{eq_j} = \rho_h A\int_0^L \psi_j^2(x)\mathrm{d}x = \rho_h AL\underbrace{\int_0^1 \psi_j^2(\xi)\mathrm{d}\xi}_{I_{1_j}} \tag{16}$$

$$k_{eq_j} = EI\int_0^L \psi_j''^2(x)\mathrm{d}x = \frac{EI}{L^3}\underbrace{\int_0^1 \psi_j''^2(\xi)\mathrm{d}\xi}_{I_{2_j}} \tag{17}$$

The equivalent damping is given by $c_{eq_j} = \alpha k_{eq_j} + \beta m_{eq_j}$. For the first mode of vibration ($j = 1$), substituting $\lambda_1 = 1.8751$, it can be shown that $I_{1_1} = 1$ and $I_{1_2} = 12.3624$. If there is a point mass of M at the tip of the cantilever, then the effective mass becomes

$$m_{eq_j} = \rho_h AL I_{1_j} + M \underbrace{\psi_j^2(1)}_{I_{3_j}} = \rho_h AL \left(I_{1_j} + \Delta M I_{3_j}\right) \tag{18}$$

For the first mode of vibration it can be shown that $I_{3_1} = 4$. The equivalent single degree of freedom model given by equation (15) is used in the rest of the document. However, the expression derived here are general and can be used if higher modes of vibration were to be employed in energy harvesting.

2.3 Derivation of the electromechanical coupling

Piezoelectric layers added to a beam is in a bimorph configuration as shown in Figure 1. The moment about the beam neutral axis produced by a voltage $V(t)$ across the piezoelectric layers may be written as

$$M_p(x,t) = \gamma_p V(t) \tag{19}$$

The constant γ_p depends on the geometry, configuration and piezoelectric device and $V(t)$ is the time-dependent voltage. For a bimorph with piezoelectric layers in the 31 configuration, with thickness h_p, width b_p and connected in parallel

$$\gamma_p = E d_{31} b_p \left(h + h_p\right) \tag{20}$$

Here h is the thickness of the beam and d_{31} is the piezoelectric constant. We assume a monolithic piezoceramic actuator perfectly bonded to the beam.

The work done by the piezoelectric patches in moving or extracting the electrical charge is

$$W_p = \int_0^{L_p} M_p(x,t)\kappa_p(x)\mathrm{d}x \tag{21}$$

where L_p is the active length of the piezoelectric material, which is assumed to be attached at the clamped end of the cantilever beam. The quantity $\kappa_p(x)$ is the curvature of the beam and this is approximately expressed by the second-derivative of the displacement. Using the approximation for κ_p we have

$$W_p(t) = \theta V(t) \tag{22}$$

where the coupling coefficient

$$\theta = \gamma_p \int_0^{L_p} \frac{\partial^2 \psi(x)}{\partial x^2}\mathrm{d}x \tag{23}$$

Considering the change to the non-dimensional variable in equation (5) and noting that we have the second-order derivative within an integral, the above equation can be simplified as

$$\theta = \frac{\gamma_p}{L}\psi'(\xi_p) \tag{24}$$

where $\xi_p = L_p/L$ is the fraction of the length of the piezo patch. Using the first mode shape, differentiating equation (4) we obtain

$$\begin{aligned}\psi'(\xi_p) = {} & ((\sin(\lambda) - \sinh(\lambda))\cosh(\lambda\,\xi_p) + (\cosh(\lambda) + \cos(\lambda))\sinh(\lambda\,\xi_p) + (\sinh(\lambda) - \sin(\lambda))\cos(\lambda\,\xi_p) \\ & + \sin(\lambda\,\xi_p)(\cosh(\lambda) + \cos(\lambda)))\,\lambda/(\cosh(\lambda) + \cos(\lambda))\end{aligned} \tag{25}$$

with $\lambda = 1.8751$. For the special case when the piezo patch covers the full length of the beam, this can be simplified as

$$\psi'(1) = \frac{2\lambda\ (\cos(\lambda)\sinh(\lambda) + \cosh(\lambda)\sin(\lambda))}{\cosh(\lambda) + \cos(\lambda)} \tag{26}$$

2.4 Incorporation of the inertial amplifier

When only the fist mode of vibration is used, the dynamics of the cantilever energy harvester can be expressed (see for example [6]) by a single degree of freedom model. In Figure 2 we show a graphical illustration of the simplified model. The inertial amplifier is obtained by attaching two small masses (m_a) with rigid (assumed to be mass-less)

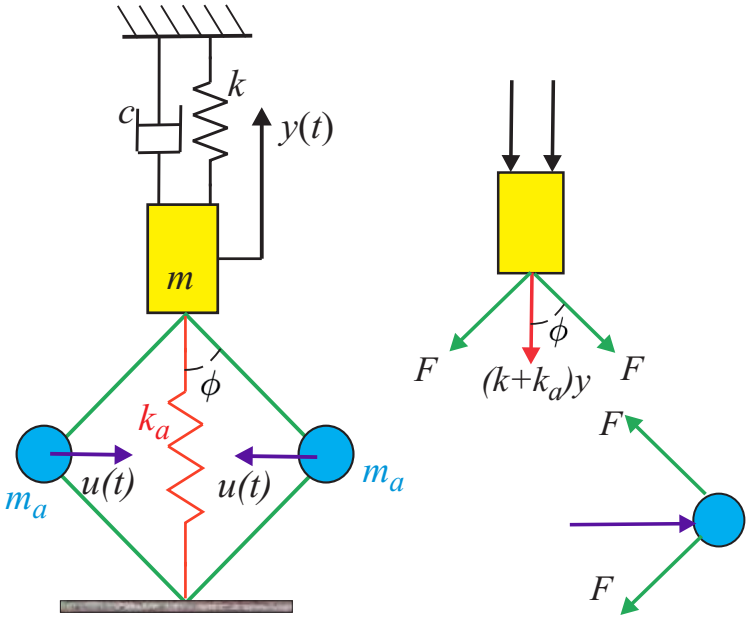

(a) Equivalent SDOF model (b) Free-body diagram

Figure 2. The equivalent single-degree-of-freedom model and the free-body diagram for energy harvesters with inertial amplifiers. The primary mass, stiffness and damping of the harvester are given by m, c and k respectively. The two small masses m_a contribute towards the inertial amplification. The amplifier angle is ϕ and the amplifier stiffness is k_a. The displacement of the primary mass and the amplifier mass are denoted by $y(t)$ and $u(t)$ respectively. The force F is the internal force within the rigid links.

rods which are pivoted on the main mass and to the ground so that they are free to rotate in a frictionless manner. The rods are placed at angle ϕ with respect to the vertical line. Additionally a spring (k_a) is attached from the main mass to the ground. In Figure 2(a), the equivalent mass, damping and stiffness are given by m, c and k and $y(t)$ is the displacement. The displacement of the amplifier mass is given by $u(t)$, which is perpendicular to the motion of the main mass. The amplifier mass would also have a vertical motion. This will be small as the mechanism will be narrow in practice due to small values of the angle ϕ. In the current analysis, the vertical motion of the amplifier mass is ignored. The free-body diagram showing the forces on the system (excluding external forces) are shown in Figure 2(b). Considering the equilibrium of the main mass we have

$$m\ddot{y}(t) + c\dot{y}(t) + (k + k_a)\, y(t) + 2F(t)\cos\phi = 0 \tag{27}$$

Here $F(t)$ is the internal force within the rigid link bars. Balancing the force arising from the motion of the amplifier mass we have

$$2F(t)\sin\phi - m_a\ddot{u}(t) = 0 \tag{28}$$

Considering the bars in Figure 2 are rigid, using the kinematic relationship of the rigid bars one deduces

$$y(t)\cos\phi = u(t)\sin\phi \quad \text{or} \quad u(t) = y(t)\cot\phi \tag{29}$$

Substituting this in equation (28) we have

$$2F(t)\sin\phi = m_a \cot\phi \ddot{y}(t) = 0 \quad \text{or} \quad 2F(t) = m_a \frac{\cot\phi}{\sin\phi}\ddot{y}(t) \tag{30}$$

Substituting this in equation (27) we obtain the equation of motion as

$$\underbrace{\left(m + m_a \cot^2\phi\right)}_{m_T}\ddot{y}(t) + c\dot{y}(t) + (k + k_a)y(t) = 0 \tag{31}$$

Here m_T is the total effective mass. For certain selection of m_a and ϕ it can be observed that the total effective mass can be significantly more than the original mass m. This amplification in the inertia has the potential of harvesting more vibration energy at a lower excitation frequency. To understand the inertial amplification, we express the effective mass in (31) as

$$\frac{m_T}{m} = 1 + \gamma_m \cot^2\phi \tag{32}$$

where the mass ratio γ_m is given by

$$\gamma_m = \frac{m_a}{m} \tag{33}$$

In Figure 3 the inertial amplification as given by equation (32) is shown in log scale. Huge amplification can be

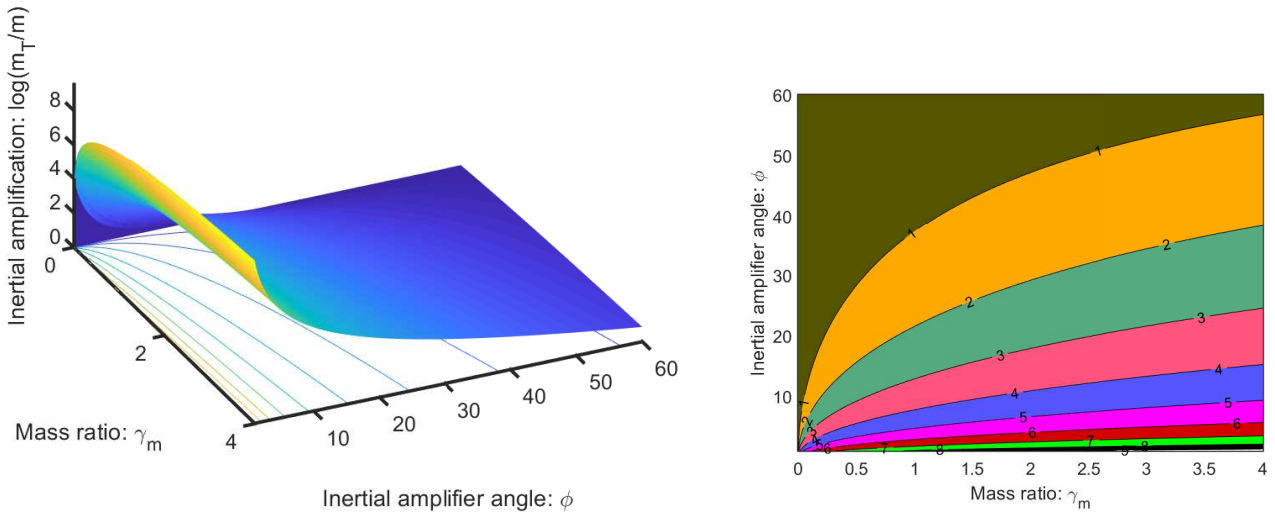

(a) Inertial amplification in the log scale

(b) Contours of the log of inertial amplification

Figure 3. Inertial amplification (in log scale) of the equivalent single-degree-of-freedom model as a function of the amplifier angle ϕ and mass-ratio γ_m.

observed for smaller values of the amplifier angle ϕ. Even when the mass ratio γ_m is less than 0.5, several orders of inertial amplification is possible with smaller amplifier angle. Therefore, the combination of the amplifier angle and mass ratio can be selected to achieve any desired inertial amplification for energy harvesting.

From Figure 3(a) we observe that the inertial amplification increases exponentially when the amplifier angle ϕ is close to zero. The two key assumptions made in the above analysis are (1) the hinge movements between the four link-bars, the three masses, the ground and the spring are frictionless, and (2) the masses of the four link-bars are negligible. When the amplifier angle ϕ becomes close to zero, the mechanism becomes very narrow and even very

small friction in the hinges will prevent it from operating properly. Keeping this in mind, in our discussions we choose $\phi > 10^\circ$. This will ensure that the assumption (1) is applicable to our model. In the other extreme case, when the amplifier angle ϕ is large, say $\phi \to 90^\circ$, the mechanism becomes very wide. In this case, significantly stronger and heavier link-bars are needed to support the weight of the amplifier masses. This will invalidate the assumption (2). For this reason, in the following discussions, the upper limit of the amplifier angle is set to $\phi < 60^\circ$. In Figure 3(a) value of the mass ratio γ_m up to 4 is used, while in Figure 3(b), the maximum value of γ_m used is 1. If $\gamma_m > 1$, the each of the inertial amplifier mass is more than the tip mass of the energy harvester. In this case heavier link-bars are needed to support the static weight of the amplifier masses even when the amplifier angle ϕ is small. This may not satisfy the assumption (2) above. Therefore, we only consider the case when the inertial amplifier mass is less than the tip mass of the harvester. Summarising, to obtain optimal parameters of the inertial amplifier, we impose the restriction of $10^\circ < \phi < 60^\circ$ and $\gamma_m < 1$ in this paper to make our predictions consistent with the assumptions made.

So far our discussion only involved the inertial properties of the harvester. The spring k_a in Figure 3 also plays a crucial role in delivering the harvested power. We define the stiffness factor Γ_k, which quantifies the overall equivalent stiffness of the dynamic system, as

$$\Gamma_k = 1 + \gamma_k \quad \text{where} \quad \gamma_k = \frac{k_a}{k} \tag{34}$$

Here γ_k is the stiffness ratio describing the stiffness of the spring k_a relative to the stiffness of the cantilever beam in the first mode of vibration. The spring k_a should be strong enough to support the static weight of the three masses so that the beam is not subjected to too much static strain. However, too much spring stiffness will result in small dynamic deformation and will diminish harvested power. The view taken in this paper is that the stiffness ratio is a variable parameter and should be optimally designed based on other parameters the model. In the next sections the impact of the stiffness ratio is assessed and methods to obtain it subjected to various optimality conditions have been proposed.

3 Energy harvesting from harmonic base excitations

In the previous section the simplified equation of motion of a piezoelectric cantilever with inertial amplifier has been developed. Here we consider energy harvesting due to harmonic base motion applied to the system as ambient excitations. Two cases of circuit configurations are considered.

3.1 Circuit without an inductor

A schematic diagram of a cantilever piezoelectric energy harvester with an inertial amplifier having a circuit without an inductor is shown in Figure 4. Next we derive mathematical expressions for the harvested power and combinations of parameters which can maximise it.

3.1.1 Quantification of the harvested power

The coupled electromechanical behaviour of the energy harvester [1] with base excitation can be expressed (see, for example [7, 8]) by linear ordinary differential equations as

$$m_T \ddot{y}(t) + c\dot{y}(t) + (k + k_a)\, y(t) - \theta v(t) = -m_T \ddot{y}_b(t) \tag{35}$$

$$C_p \dot{v}(t) + \frac{1}{R_l} v(t) + \theta \dot{y}(t) = 0 \tag{36}$$

Here m_T is the total effective mass, $y(t)$ is the relative motion of the system with respect to the base excitation $y_b(t)$, $v(t)$ is the voltage, R_l is the load resistance, C_p is the capacitance of the piezoelectric layer, t is the time and θ is the electromechanical coupling.

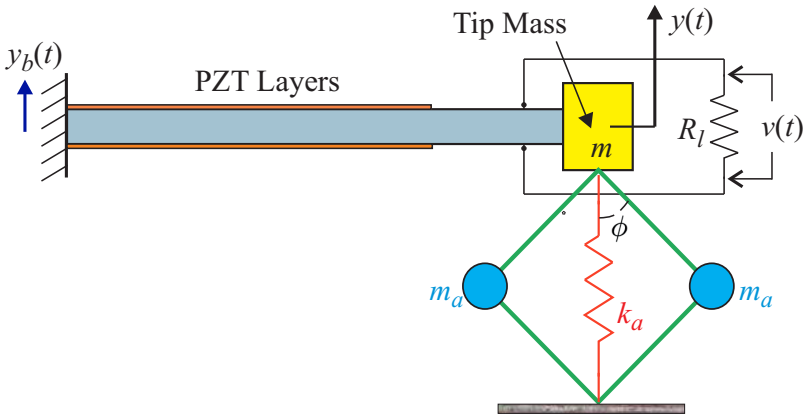

Figure 4. A cantilever piezoelectric energy harvester with an inertial amplifier having a circuit without an inductor. R_l is the load resistance of the harvesting circuit. The source of the ambient energy is through the base-excitation $y_b(t)$. The displacement of the primary mass and the voltage generated due to the strain in the piezoelectric layers are denoted by $y(t)$ and $v(t)$ respectively.

We consider a deterministic harmonic base excitation so that

$$y_b(t) = Y_b e^{\mathrm{i}\omega t} \tag{37}$$

Here ω is the driving frequency and i is the unit imaginary number $\mathrm{i} = \sqrt{-1}$. Transforming equations (35) and (36) into the frequency domain and dividing the first equation by m and the second equation by C_p we obtain

$$\left(-\omega^2\left(1+\gamma_m\cot^2\phi\right)+2\mathrm{i}\omega\zeta\omega_n+\omega_n^2\left(1+\gamma_k\right)\right)Y(\mathrm{i}\omega)-\frac{\theta}{m}V(\mathrm{i}\omega)=\omega^2\left(1+\gamma_m\cot^2\phi\right)Y_b \tag{38}$$

$$\mathrm{i}\omega\frac{\theta}{C_p}Y(\mathrm{i}\omega)+\left(\mathrm{i}\omega+\frac{1}{C_pR_l}\right)V(\mathrm{i}\omega)=0 \tag{39}$$

Here $Y(\mathrm{i}\omega)$ and $V(\mathrm{i}\omega)$ are respectively the Fourier transforms of $y(t)$ and $v(t)$ and γ_m is the mass ratio defined in equation (33). The natural frequency of the harvester (ω_n) and the damping factor (ζ) are defined as

$$\omega_n=\sqrt{\frac{k}{m}} \quad \text{and} \quad \zeta=\frac{c}{2m\omega_n} \tag{40}$$

Dividing the equation (38) by ω_n^2 and equation (39) by ω_n and writing in a matrix form one has

$$\begin{bmatrix}\left(\Gamma_k-\Omega^2\Gamma_m\right)+2\mathrm{i}\Omega\zeta & -\frac{\theta}{k}\\ \mathrm{i}\Omega\frac{\alpha\theta}{C_p} & (\mathrm{i}\Omega\alpha+1)\end{bmatrix}\begin{Bmatrix}Y(\mathrm{i}\Omega)\\ V(\mathrm{i}\Omega)\end{Bmatrix}=\begin{Bmatrix}\Omega^2\Gamma_mY_b\\ 0\end{Bmatrix} \tag{41}$$

Here the dimensionless frequency and the time constant are defined as

$$\Omega=\frac{\omega}{\omega_n} \quad \text{and} \quad \alpha=\omega_nC_pR_l \tag{42}$$

Note that α is the time constant of the first order electrical system, non-dimensionalized using the natural frequency of the mechanical system. We also define the non-dimensional mass factor of the inertial amplifier as

$$\Gamma_m=1+\gamma_m\cot^2\phi \tag{43}$$

Inverting the coefficient matrix, the displacement and voltage in the frequency domain can be obtained as

$$\begin{Bmatrix} Y(\mathrm{i}\Omega) \\ V(\mathrm{i}\Omega) \end{Bmatrix} = \frac{1}{\Delta_1(\mathrm{i}\Omega)} \begin{bmatrix} (\mathrm{i}\Omega\alpha + 1) & \frac{\theta}{k} \\ -\mathrm{i}\Omega\frac{\alpha\theta}{C_p} & \left(\Gamma_k - \Omega^2\Gamma_m\right) + 2\mathrm{i}\Omega\zeta \end{bmatrix} \begin{Bmatrix} \Omega^2\Gamma_m Y_b \\ 0 \end{Bmatrix} \tag{44}$$

In the above equation, the determinant of the coefficient matrix is given by

$$\Delta_1(\mathrm{i}\Omega) = \Gamma_m(\mathrm{i}\Omega)^3\alpha + (2\,\zeta\,\alpha + \Gamma_m)\,(\mathrm{i}\Omega)^2 + \left((\kappa^2 + (1+\gamma_k))\alpha + 2\,\zeta\right)(\mathrm{i}\Omega) + (1+\gamma_k) \tag{45}$$

and the non-dimensional electromechanical coupling coefficient is defined as

$$\kappa^2 = \frac{\theta^2}{kC_p} \tag{46}$$

From equation (44) we obtain the dynamic response and the voltage output of the system due to the harmonic base excitation as

$$Y(\mathrm{i}\Omega) = \frac{(\mathrm{i}\Omega\alpha + 1)\,\Omega^2\Gamma_m Y_b}{\Delta_1(\mathrm{i}\Omega)} \tag{47}$$

$$\text{and} \quad V(\mathrm{i}\Omega) = -\mathrm{i}\Omega\frac{\alpha\theta}{C_p}\frac{\Omega^2\Gamma_m Y_b}{\Delta_1(\mathrm{i}\Omega)} \tag{48}$$

It is convenient to view the response quantities in a non-dimensional form. The harvested power is given by

$$P(\Omega) = \frac{V^2(\Omega)}{R_l} \tag{49}$$

As R_l is a constant, to obtain an expression of the power in a non-dimensional form, it is necessary to non-dimentionalise the voltage only. This can be achieved in various ways. For analytical convenience, the voltage at $\Omega = 1$ when the damping is zero and without the inertial amplifier is considered to be used for the normalisation

$$V_0 = V(\mathrm{i}\Omega)|_{\{\Omega=1,\zeta=0,\gamma_m=0,\gamma_k=0\}} = \frac{-\mathrm{i}\frac{\alpha\theta}{C_p}Y_b}{\mathrm{i}\alpha\kappa^2} = -\frac{\theta Y_b}{C_p\kappa^2} \tag{50}$$

Using this, we obtain the non-dimensional voltage response as

$$\widehat{V}(\mathrm{i}\Omega) = \frac{V(\mathrm{i}\Omega)}{V_0} = \alpha\kappa^2\frac{\mathrm{i}\Omega^3\Gamma_m}{\Delta_1(\mathrm{i}\Omega)} \tag{51}$$

The non-dimensional power is therefore given by

$$\widehat{P}(\Omega) = \frac{P(\Omega)}{P_0} = \left|\frac{V(\mathrm{i}\Omega)}{V_0}\right|^2 = \left|\widehat{V}(\mathrm{i}\Omega)\right|^2 \tag{52}$$

For the case of harmonic base excitation, a key interest is the variation of the harvested power as function of driving frequency of the base excitation. To gain physical insights, the results obtained so far is applied numerically to an example problem. Table 1 gives the parameters of the system for the simulations (taken from reference [9]). For these values of the parameters, we obtain $V_0 = 897.15$ V for $Y_b = 1$ mm. Depending on the system parameters, the value of V_0 will change significantly. Throughout this study, the results are shown in a non-dimensional manner for generality. The actual values can be obtained simply by multiplying the corresponding normalisation factors.

The non-dimensional harvested power given by equation (52) is plotted as a function of the non-dimensional frequency in Figure 5. Two sets of parameters are considered for the inertial amplifier, namely $\gamma_m = 0.2$, $\gamma_k = 1$, $\phi = 10^\circ$

Table 1. Parameter values used in the simulation

Parameter	Value	Unit
m	9.12×10^{-3}	kg
k	4.1×10^{3}	N/m
c	0.135	Ns/m
R_l	3×10^{4}	Ohm
C_p	4.3×10^{-8}	F
θ	-4.57×10^{-3}	N/V
ω_n	670.49	rad/s
ζ	0.011	–
α	0.8649	–
κ^2	0.1185	–

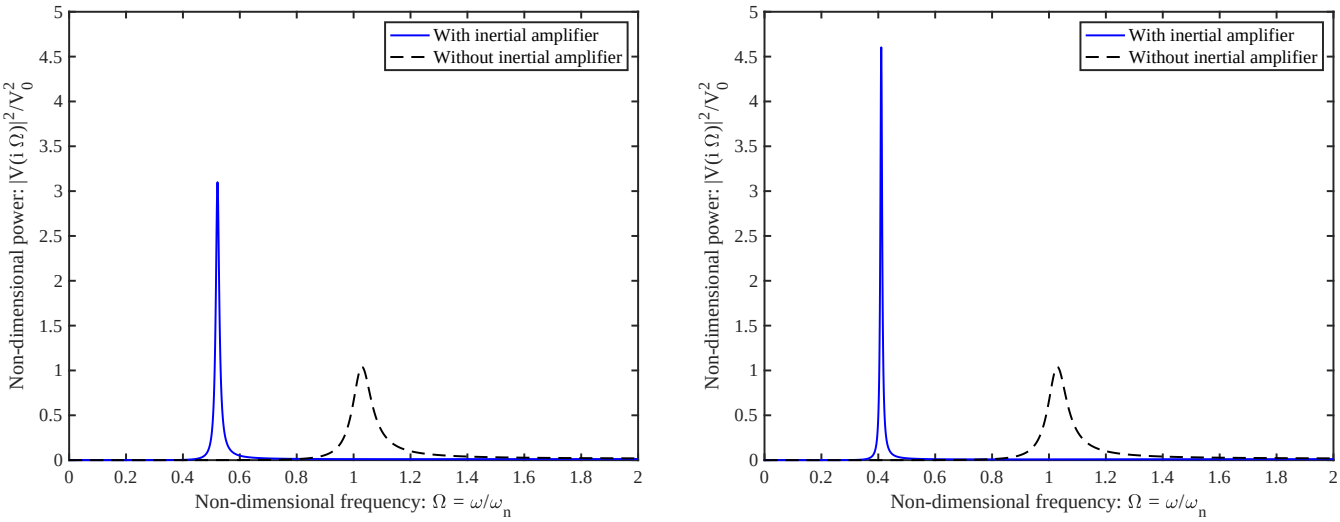

(a) Inertial amplifier with $\gamma_m = 0.2$, $\gamma_k = 1$, $\phi = 10^\circ$

(b) Inertial amplifier with $\gamma_m = 1$, $\gamma_k = 1.5$, $\phi = 15^\circ$

Figure 5. The non-dimensional power of a harvester without an inductor ($\zeta = 0.011$, $\alpha = 0.8649$, $\kappa^2 = 0.1185$) as a function of non-dimensional frequency. Powers obtained from the classical harvester without an inertial amplifier and the proposed harvester with two different inertial amplifier configurations are shown for comparison. Powers obtained from the proposed harvesters are 3 and 4.5 times more than the classical harvester at 50% and 60% lower frequencies.

and $\gamma_m = 1$, $\gamma_k = 0.6$, $\phi = 15^\circ$. Both demonstrate higher harvested power at a lower frequency compared to the classical case without any inertial amplifier. The system in Figure 5(b) shows relatively higher harvested power at a relatively lower frequency compared to the system Figure 5(a). As the harvested power is significantly depended on the parameters of the inertial amplifier, next we aim to obtain optimal parameters to maximise the power output of the energy harvester.

3.1.2 Optimisation of the harvested power

The first step to maximise the harvested power is to determine at which frequency value the maxima of the power occurs. For lightly damped systems without the inertial amplifier, the harvested power peaks about $\Omega \approx 1$. To obtain the frequency at which the harvested power peaks we set derivative of the normalised power given in equation (52) with respect to the normalised frequency-square to zero

$$\frac{\partial \widehat{P}(\Omega^2)}{\partial \Omega^2} = 0 \tag{53}$$

Simplifying this we obtain the necessary condition as

$$\underbrace{-2\Gamma_m^2\alpha^2}_{a_1}(\Omega^2)^3 + \underbrace{\left(2\Gamma_m\alpha^2\kappa^2 + 2\Gamma_m\Gamma_k\alpha^2 - 4\alpha^2\zeta^2 - \Gamma_m^2\right)}_{a_2}(\Omega^2)^2 + \underbrace{\Gamma_k^2}_{a_4} = 0 \tag{54}$$

This is a cubic equation in Ω^2. In general there is one real solution and one complex conjugate pair of solutions. The positive real solution can be given exactly as

$$\Omega^2_{\max} = -\frac{1}{3a_1}\left(a_2 + C + \frac{\Delta_0}{C}\right) \tag{55}$$

Here $a_j, j = 1, \cdots, 4$ are the coefficients of the polynomial in the order of decreasing power (note that $a_3 = 0$) with

$$\Delta_0 = a_2^2 - 3a_1a_3, \Delta_1 = 2a_2^3 - 9a_1a_2a_3 + 27a_1^2a_4 \quad \text{and} \quad C = \sqrt[3]{\frac{\Delta_1 \pm \sqrt{\Delta_1^2 - 4\Delta_0^3}}{2}} \tag{56}$$

The expression in equation (55) us exact but requires several calculations and not physically intuitive. From the equation of motion (38) we conjecture that the maximum power occurs around $\Omega^2 \approx \frac{\Gamma_k}{\Gamma_m}$. Using this and assuming that damping is small such that $\zeta^2 \to 0$, we can obtain a first-order approximation of the optimal frequency point as

$$\Omega^2_{\max} \approx \frac{\Gamma_k}{\Gamma_m}\left[1 + \frac{\alpha^2\kappa^2}{\Gamma_m + \alpha^2(\Gamma_k - 2\kappa^2)}\right] \tag{57}$$

The non-dimensional frequency for the maximum harvested power is therefore a function of the inertial amplifier parameters, time constant and electromechanical coupling coefficient.

In Figure 6 the non-dimensional power is shown for two different inertial amplifiers. Five values of the damping factors of the energy harvesters have been considered. They range from undamped to a damping factor of 20%. As expected, less damping in the harvester leads to more harvested power from the harmonic base excitation. The value of $\Omega_{\max}$ obtained from equation (57) is shown in Figure 6 by a '*'. It closely matches with the frequency for which the harvested power is maximum for all the five damping values. The non-dimensional frequency for the maximum power obtained from (57) are respectively 0.5213 and 0.4103. Comparing with the exact results, it was verified that for all the damping values, the frequency for the maximum power does not change significantly. Note that for both the cases this is significantly lower than the classical harvester without an inertial amplifier, for which $\Omega_{\max}$ is close to 1. This clearly demonstrates that the maximum power is harvested at a lower frequency compared the classical harvester.

To gain further understanding on how the parameters of the inertial amplifier impact the frequency for the maximum power, in Figure 7 we show the contour lines of $\Omega_{\max}$ as functions of the stiffness ratio γ_k and inertial amplifier angle ϕ. Four values of the mass ratio γ_m and a damping factor of $\zeta = 0.011$ have been used. We also show the contour line of the frequency for the maximum power for the classical energy harvester without the inertial amplifier in the same plots. This is close to 1 and therefore any contour lines below this value show the parameter combinations for

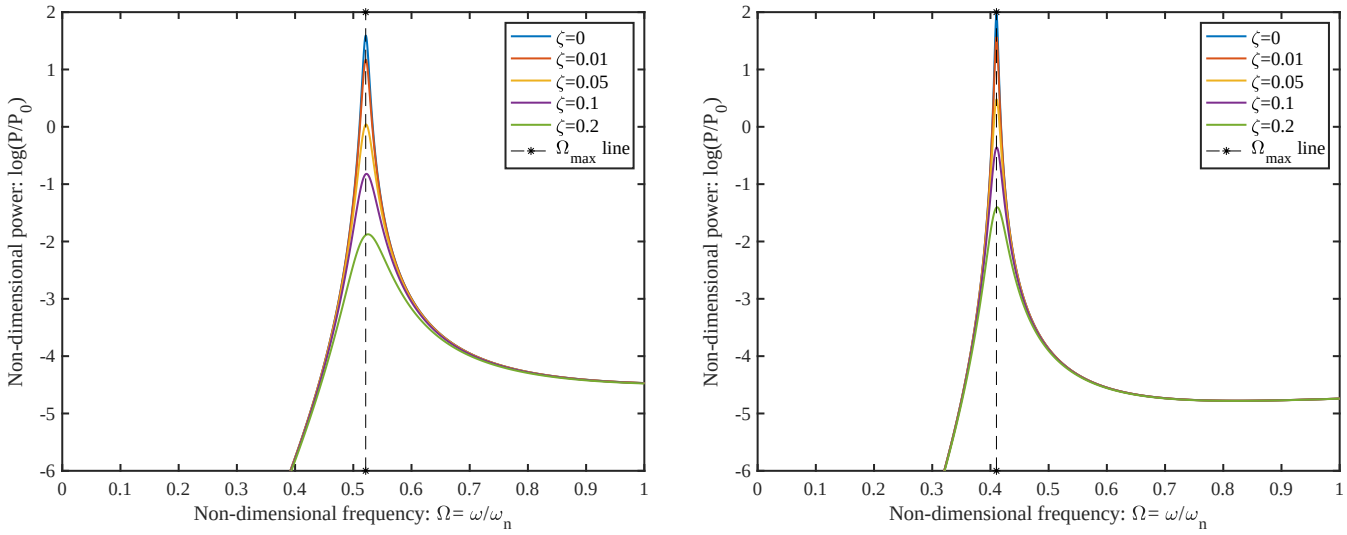

(a) Inertial amplifier with $\gamma_m = 0.2$, $\gamma_k = 1$, $\phi = 10^\circ$

(b) Inertial amplifier with $\gamma_m = 1$, $\gamma_k = 1.5$, $\phi = 15^\circ$

Figure 6. The non-dimensional power of a harvester without an inductor ($\alpha = 0.8649$, $\kappa^2 = 0.1185$) as a function of the non-dimensional frequency for five selected values of damping factors. The value of the frequency of maximum power ($\Omega_{\max}$) obtained from equation (57) is shown in Figure 6 by a '*'. Five values of the damping factors of the energy harvesters have been considered for illustration.

which maximum power occurs below the classical case. A key observation is that for larger inertial amplifier mass (i.e., larger γ_m), a wider angle ϕ can be used to achieve a lower maximum frequency vale. For lower values of ϕ, $\Omega_{\max}$ is not very sensitive with γ_k.

The non-dimensional maximum harvested power is shown in Figure 8 as a function of the stiffness ratio γ_k and inertial amplifier angle ϕ for four different values of the mass ratio. The maximum power is obtained by computing the power at frequency values shown in Figure 6. We also show the contour line of the maximum power for the classical energy harvester without the inertial amplifier in the same plots. For most parameter combinations, the harvested power for the proposed system with inertial amplifier is more than the classical harvester. Increasing the stiffness in general leads to a higher harvested power. We also observe that the harvested power does not change with ϕ significantly beyond the inertial amplifier angle of 45°.

Form Figure 8 observe that a higher stiffness ratio γ_k leads to a higher harvested power. However, Figure 7 shows that higher stiffness ratio γ_k also leads to higher values of the frequency for the maximum power, which is not ideal for low-frequency energy harvesting. Therefore, the parameters should be selected for an optimal balance between maximum power and minimum frequency. Equation (57) along with Figures 7 and 8 can give a practical approach towards selecting optimal parameters. We select $\eta < 1$ as the desired normalised frequency value for the maximum harvested power. One can equate this quantity to the exact expression of the maximum frequency in (55). However, to simplify the analytical expression, the approximate expression in equation (57) has been used. Therefore substituting

$$\eta = \omega_{\max} \tag{58}$$

as the target frequency for the maximum power, from equation (57) we have

$$\Gamma_m \eta^2 - \Gamma_k \left[1 + \frac{\alpha^2 \kappa^2}{\Gamma_m + \alpha^2 (\Gamma_k - 2\kappa^2)} \right] = 0 \tag{59}$$

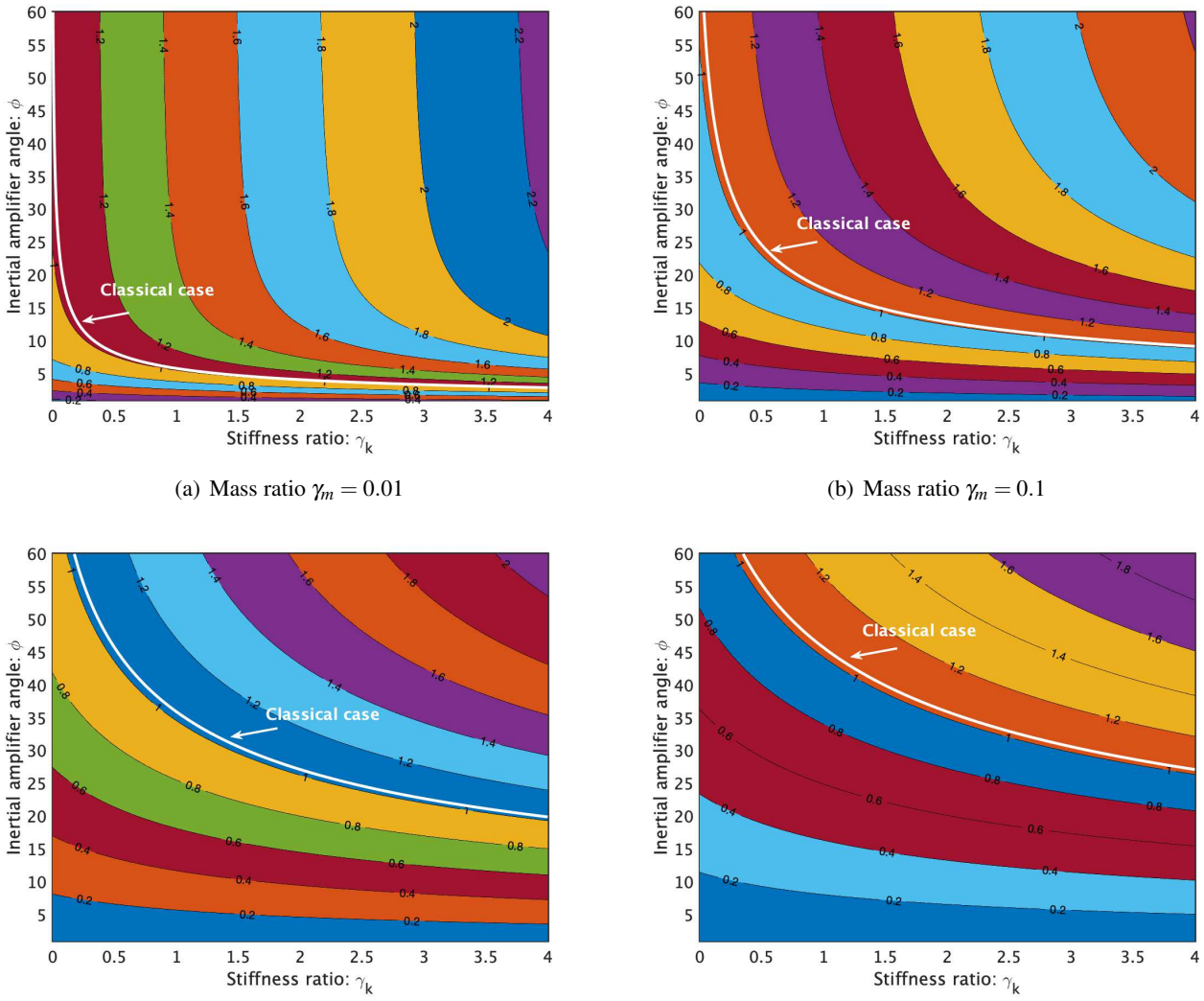

(a) Mass ratio $\gamma_m = 0.01$

(b) Mass ratio $\gamma_m = 0.1$

(c) Mass ratio $\gamma_m = 0.5$

(d) Mass ratio $\gamma_m = 1.0$

Figure 7. Contours of non-dimensional frequency for maximum power of a harvester without an inductor ($\zeta = 0.011$, $\alpha = 0.8649$, $\kappa^2 = 0.1185$) as a function of the stiffness ratio γ_k and inertial amplifier angle ϕ. The non-dimensional frequency for maximum power for the equivalent classical harvester without an inertial amplifier is a constant (function of the electrical parameters only) and shown by a line as indicated. Contour lines below the classical line indicate that the maximum power of a harvester with an inertial amplifier takes place at a lower frequency. Higher values of the mass ratio γ_m and smaller amplifier angles ($\phi \lessapprox 15^\circ$) ensure this fact for any stiffness ratio.

Simplifying this equation we obtain

$$\Gamma_k{}^2\alpha^2 + \left(\left(-\eta^2\Gamma_m - \kappa^2\right)\alpha^2 + \Gamma_m\right)\Gamma_k + 2\Gamma_m\alpha^2\eta^2\kappa^2 - \Gamma_m{}^2\eta^2 = 0 \tag{60}$$

This is a quadratic equation in Γ_k and taking the positive solution, the optimal value of the stiffness ratio (note that

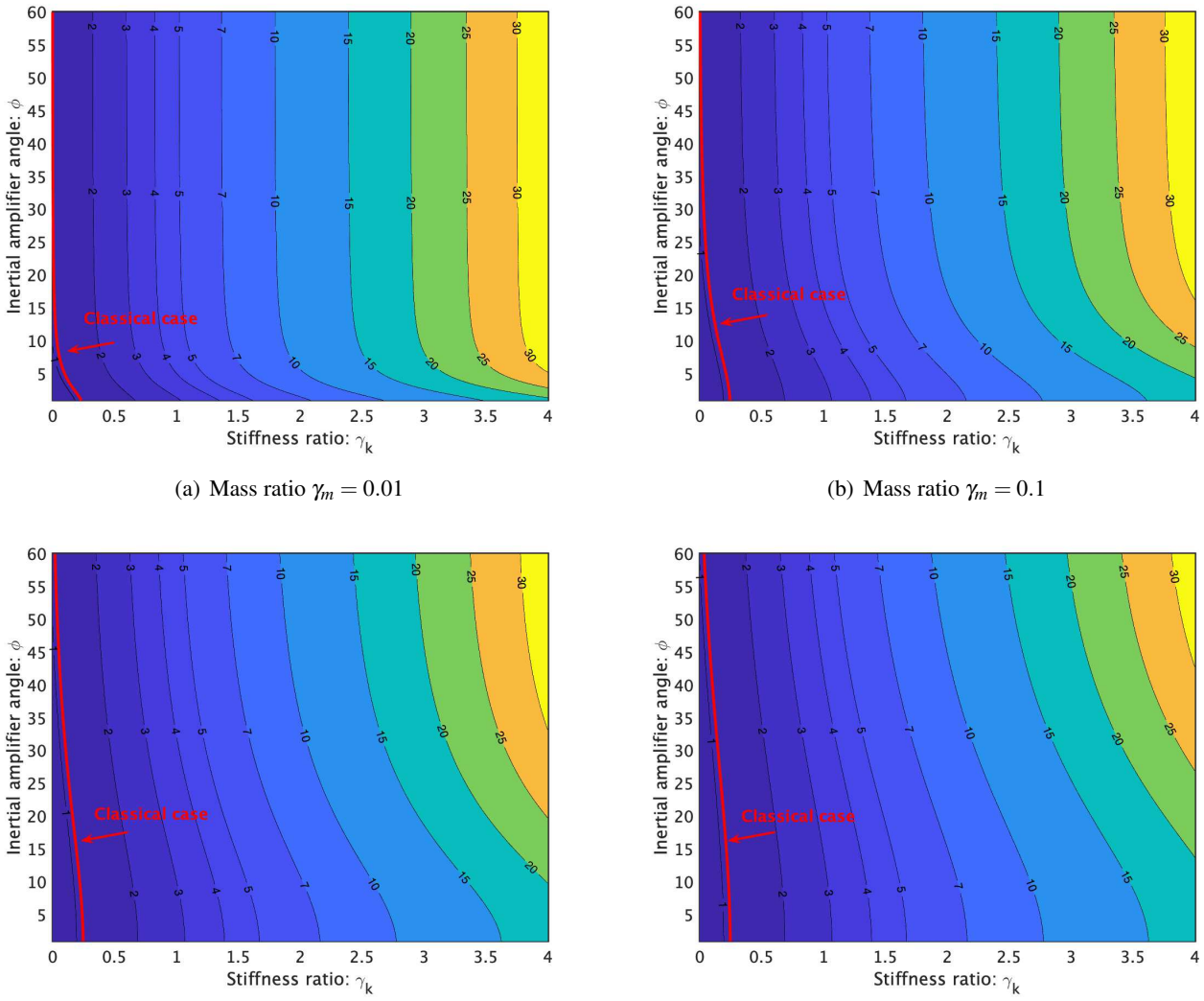

(a) Mass ratio $\gamma_m = 0.01$

(b) Mass ratio $\gamma_m = 0.1$

(c) Mass ratio $\gamma_m = 0.5$

(d) Mass ratio $\gamma_m = 1.0$

Figure 8. Contours of non-dimensional maximum power of a harvester without an inductor ($\zeta = 0.011$, $\alpha = 0.8649$, $\kappa^2 = 0.1185$) as a function of the stiffness ratio γ_k and inertial amplifier angle ϕ. The non-dimensional maximum power for the equivalent classical harvester without an inertial amplifier is a constant (slightly more than 1) and shown by the indicated line. Contour lines above the classical line indicate that the maximum power of a harvester with an inertial amplifier is higher for the respective parameter combinations. Higher stiffness ratio γ_k leads to higher harvested power. However, the harvested power does not change significantly for larger amplifier angles, $\phi \gtrapprox 30°$. Except for very small values of the stiffness ratio γ_k, maximum power obtained from the proposed harvester is always more than the classical harvester.

$\gamma_k = \Gamma_k - 1$) can be obtained as

$$\gamma_k = \frac{\sqrt{\left(\eta^2\alpha^2+1\right)^2{\Gamma_m}^2 + \left(-6\alpha^4\eta^2 - 2\alpha^2\right)\kappa^2\Gamma_m + \alpha^4\kappa^4} + \left(\Gamma_m\eta^2 + \kappa^2 - 2\right)\alpha^2 - \Gamma_m}{2\alpha^2} \tag{61}$$

Therefore, from the preceding equation, given a target frequency for maximum power $\eta < 1$, one can explicitly choose the stiffness ratio given the parameters of the harvesting circuit and inertial amplifier parameters such as γ_k

and ϕ. In Figure 9 we show the contours of the optimal non-dimensional stiffness stiffness ratio γ_k from equation (60) for different values of the inertial amplifier angle ϕ and target frequency for maximum power η. Results for

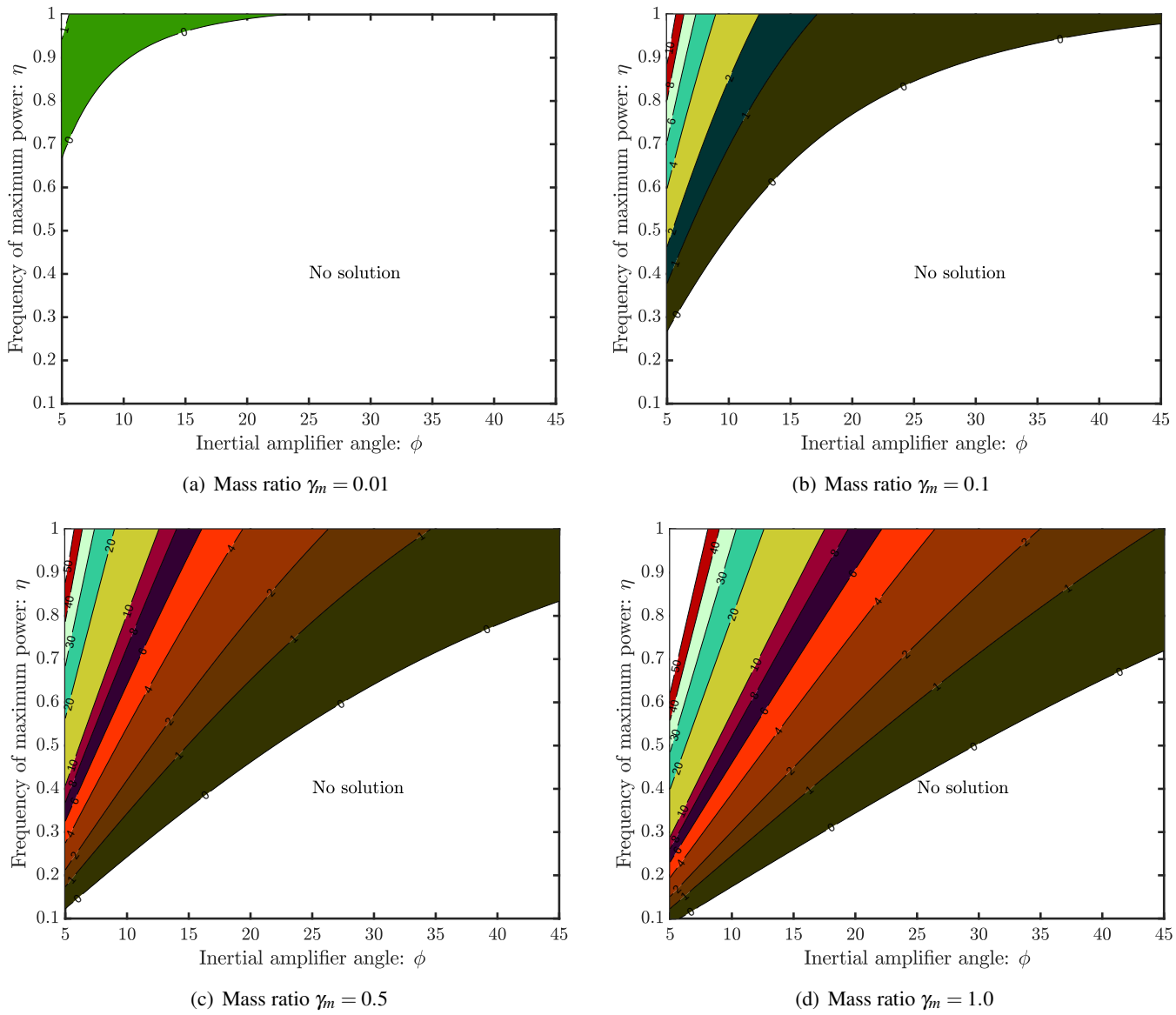

(a) Mass ratio $\gamma_m = 0.01$

(b) Mass ratio $\gamma_m = 0.1$

(c) Mass ratio $\gamma_m = 0.5$

(d) Mass ratio $\gamma_m = 1.0$

Figure 9. Contours of the optimal non-dimensional stiffness ratio γ_k for of a harvester without an inductor ($\zeta = 0.011$, $\alpha = 0.8649$, $\kappa^2 = 0.1185$) as a function of the target frequency for the maximum power η and inertial amplifier angle ϕ. The empty region marked above show the parameter combination when t is not possible to obtain a real and positive value of the stiffness ratio.

four different values of the mass ratio are shown in Figure 9. When the mass ratio γ_m is small, say $\gamma_m = 0.01$ (that is only 1% of the tip mass), then it is not possible to obtain a real and positive value of the spring stiffness for a large number of parameter combinations as shown by the empty region in Figure 9(a). For larger inertial amplifier mass, more parameter combinations give physically realistic value of the spring stiffness for a target frequency for maximum power harvesting as seen in Figure 9(d). From these plots we also observe that if the inertial amplifier stiffness value to be kept low and a lower frequency for maximum power harvesting is needed, the mass of the inertial amplifier

should be higher.

If the stiffness of the inertial amplifier is known or has been selected, then equation (59) can also be used to obtain γ_m and ϕ for maximum power at a prescribed target frequency value η. Solving the resulting quadratic equation we obtain

$$\gamma_m \cot^2\phi = \frac{\sqrt{\eta^4\left(-2\kappa^2+\Gamma_k\right)^2\alpha^4+2{\Gamma_k}^2\alpha^2\eta^2+{\Gamma_k}^2}+\left(-2+\left(2\kappa^2-\Gamma_k\right)\alpha^2\right)\eta^2+\Gamma_k}{2\eta^2} \tag{62}$$

This allows one to choose the optimal combination of γ_m and ϕ for maximum power at frequency η. Next, we consider the case when the electrical circuit has an inductor.

3.2 Circuit with an inductor

A schematic diagram of a cantilever piezoelectric energy harvester with an inertial amplifier having a circuit with an inductor is shown in Figure 10. Next we derive mathematical expressions for the harvested power and combinations

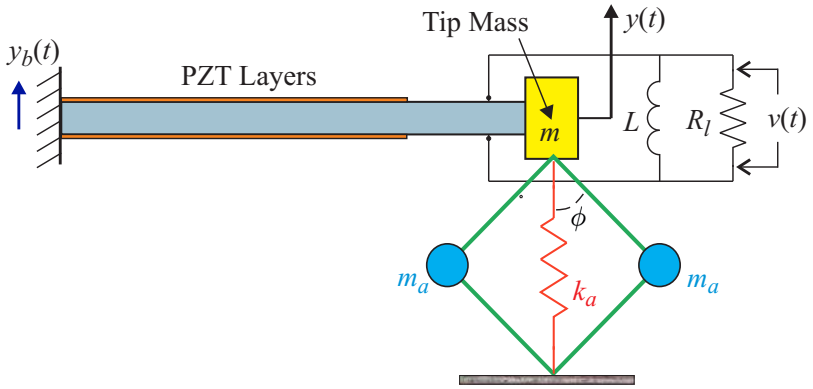

Figure 10. A cantilever piezoelectric energy harvester with an inertial amplifier having a circuit with an inductor. R_l is the load resistance and L is the inductor of the harvesting circuit. The source of the ambient energy is through the base-excitation $y_b(t)$. The displacement of the primary mass and the voltage generated due to the strain in the piezoelectric layers are denoted by $y(t)$ and $v(t)$ respectively.

of parameters which can maximise it.

3.2.1 Quantification of the harvested power

Piezoelectric vibration energy harvester comprising a circuit with an inductor is shown in Figure 10. For this case the electrical equation (see for example, [10]) becomes

$$C_p\ddot{v}(t)+\frac{1}{R_l}\dot{v}(t)+\frac{1}{L_i}v(t)+\theta\ddot{y}(t)=0 \tag{63}$$

where L_i is the inductance of the circuit. The mechanical equation is the same as given in equation (35).

Transforming equation (63) into the frequency domain and dividing by $C_p\omega_n^2$ one has

$$-\Omega^2\frac{\theta}{C_p}Y(\mathrm{i}\omega)+\left(-\Omega^2+\mathrm{i}\Omega\frac{1}{\alpha}+\frac{1}{\beta}\right)V(\mathrm{i}\omega)=0 \tag{64}$$

where the normalised inductor parameter is defined as

$$\beta=\omega_n^2L_iC_p \tag{65}$$

and is the ratio of the mechanical to electrical natural frequencies. Similar to equation (41), this equation can be written in matrix form with the equation of motion of the mechanical system (38) as

$$\begin{bmatrix} \left(\Gamma_k - \Omega^2\Gamma_m\right) + 2\mathrm{i}\Omega\zeta & -\frac{\theta}{k} \\ -\Omega^2\frac{\alpha\beta\theta}{C_p} & \alpha\left(1-\beta\Omega^2\right) + \mathrm{i}\Omega\beta \end{bmatrix} \begin{Bmatrix} Y(\mathrm{i}\omega) \\ V(\mathrm{i}\omega) \end{Bmatrix} = \begin{Bmatrix} \Omega^2\Gamma_m Y_b \\ 0 \end{Bmatrix} \tag{66}$$

Inverting the coefficient matrix, the displacement and voltage in the frequency domain can be obtained as

$$\begin{Bmatrix} Y(\mathrm{i}\omega) \\ V(\mathrm{i}\omega) \end{Bmatrix} = \frac{1}{\Delta_2} \begin{bmatrix} \alpha\left(1-\beta\Omega^2\right) + \mathrm{i}\Omega\beta & \frac{\theta}{k} \\ \Omega^2\frac{\alpha\beta\theta}{C_p} & \left(\Gamma_k - \Omega^2\Gamma_m\right) + 2\mathrm{i}\Omega\zeta \end{bmatrix} \begin{Bmatrix} \Omega^2\Gamma_m Y_b \\ 0 \end{Bmatrix} \tag{67}$$

where the determinant of the coefficient matrix is

$$\Delta_2(\mathrm{i}\Omega) = (\mathrm{i}\Omega)^4\beta\,\alpha\Gamma_m + \beta\left(2\,\zeta\,\alpha + \Gamma_m\right)(\mathrm{i}\Omega)^3 + \left(\left(\left(k^2+\Gamma_k\right)\beta + \Gamma_m\right)\alpha + 2\,\beta\,\zeta\right)(\mathrm{i}\Omega)^2 + \left(\Gamma_k\beta + 2\,\alpha\,\zeta\right)(\mathrm{i}\Omega) + \Gamma_k\alpha \tag{68}$$

From equation (67) we obtain the dynamic response and the voltage output of the system due to the harmonic base excitation as

$$Y(\mathrm{i}\Omega) = \frac{\left(\alpha\left(1-\beta\Omega^2\right) + \mathrm{i}\Omega\beta\right)\Omega^2\Gamma_m Y_b}{\Delta_2(\mathrm{i}\omega)} \tag{69}$$

$$\text{and} \quad V(\mathrm{i}\Omega) = \frac{\Omega^2\frac{\alpha\beta\theta}{C_p}\Omega^2\Gamma_m Y_b}{\Delta_2(\mathrm{i}\omega)} \tag{70}$$

As the previous case, the voltage at $\Omega = 1$ when the damping is zero and without the inertial amplifier is considered to be used for the normalisation

$$V_0 = V(\mathrm{i}\Omega)\big|_{\{\Omega=1,\zeta=0,\gamma_m=0,\gamma_k=0\}} = \frac{\frac{\alpha\beta\theta}{C_p}Y_b}{-\alpha\beta\,\kappa^2} = -\frac{\theta Y_b}{C_p\kappa^2} \tag{71}$$

Using this, we obtain the non-dimensional voltage response as

$$\widehat{V}(\mathrm{i}\Omega) = \frac{V(\mathrm{i}\Omega)}{V_0} = \alpha\beta\,\kappa^2\Omega^2\frac{(\mathrm{i}\Omega)^2}{\Delta_2(\mathrm{i}\Omega)} \tag{72}$$

Using this expression, the non-dimensional power can be obtained from (52). Next we investigate the impact of the inertial amplifier on the harvested power.

The non-dimensional harvested power using the expression of the voltage in (72) is plotted as a function of the non-dimensional frequency in Figure 11. Two sets of parameters are considered for the inertial amplifier, namely $\gamma_m = 0.2$, $\gamma_k = 1$, $\phi = 10^\circ$ and $\gamma_m = 1$, $\gamma_k = 0.6$, $\phi = 15^\circ$. The value of the non-dimensional inductor constant is assumed to be $\beta = 1.0$. Both demonstrate higher harvested power at a lower frequency compared to the classical case without any inertial amplifier. The system in Figure 11(b) shows relatively higher harvested power at a relatively lower frequency compared to the system Figure 11(a). As the harvested power significantly depended on the parameters of the inertial amplifier, next we aim to obtain optimal parameters to maximise the power output of the energy harvester.

3.2.2 Optimisation of the harvested power

To obtain the frequency at which the harvested power peaks, we consider the normalised power given by equation (52) with the voltage expression in (72) as

$$\widehat{P}(\Omega) = (\alpha\beta\,\kappa^2)^2\frac{(\Omega)^8}{\Delta_2(\mathrm{i}\Omega)\Delta_2^*(\mathrm{i}\Omega)} \tag{73}$$

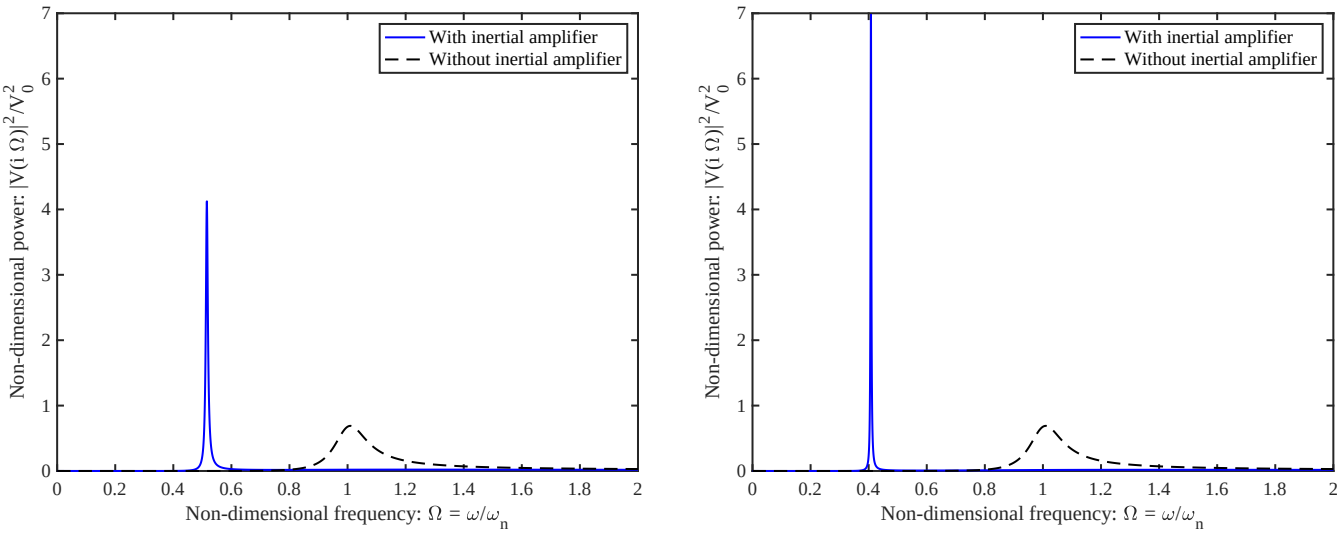

(a) Inertial amplifier with $\gamma_m = 0.2$, $\gamma_k = 1$, $\phi = 10^\circ$

(b) Inertial amplifier with $\gamma_m = 1$, $\gamma_k = 0.6$, $\phi = 15^\circ$

Figure 11. The non-dimensional power of a harvester with an inductor ($\zeta = 0.011$, $\alpha = 0.8649$, $\kappa^2 = 0.1185$, $\beta = 1.0$) as a function of non-dimensional frequency. Powers obtained from the classical harvester without an inertial amplifier and the proposed harvester with two different inertial amplifier configurations are shown for comparison. Powers obtained from the proposed harvesters are approximately 4 and 7 times more than the classical harvester at 50% and 60% lower frequencies.

Here $(\bullet)^*$ denotes complex conjugation. We set derivative of the normalised power given by equation (73) with respect to the normalised frequency-square to zero

$$\frac{\partial \widehat{P}(\Omega^2)}{\partial \Omega^2} = 0 \tag{74}$$

Simplifying this we obtain the necessary condition as a fourth-order polynomial in Ω^2

$$a_1(\Omega^2)^4 + a_2(\Omega^2)^3 + a_3(\Omega^2)^2 + a_4(\Omega^2) + a_5 = 0 \tag{75}$$

where

$$\begin{aligned} a_1 &= -3{\Gamma_m}^2\alpha^2\beta^2, a_2 = 4\Gamma_m\alpha^2\beta^2\kappa^2 + 4\Gamma_m\Gamma_k\alpha^2\beta^2 + 4{\Gamma_m}^2\alpha^2\beta - 2{\Gamma_m}^2\beta^2 \\ a_3 &= -\alpha^2\beta^2\kappa^4 - 2\Gamma_k\alpha^2\beta^2\kappa^2 - 2\Gamma_m\alpha^2, a_4 = 0, a_5 = {\Gamma_k}^2\alpha^2 \end{aligned} \tag{76}$$

The four solutions of equation (75) can be given in closed-from as

$$\Omega^2_{1,2,3,4} = -\frac{a_2}{4a_1} \mp S \pm \frac{1}{2}\sqrt{-4S^2 - 2p + \frac{q}{S}} \tag{77}$$

Here

$$p = \frac{8a_1a_3 - 3a_2^2}{8a_1^2}, q = \frac{a_2^3 - 4a_1a_2a_3 + 8a_1^2a_4}{8a_1^3}, \tag{78}$$

$$S = \frac{1}{2}\sqrt{-\frac{2}{3}p + \frac{1}{3a_1}\left(Q + \frac{\Delta_0}{Q}\right)}, Q = \sqrt[3]{\frac{\Delta_1 + \sqrt{\Delta_1^2 - 4\Delta_0^3}}{2}} \tag{79}$$

$$\Delta_0 = a_3^2 - 3a_2a_4 + 12a_1a_5, \Delta_1 = 2a_3^3 - 9a_2a_3a_4 + 27a_2^2a_5 + 27a_1a_4^2 - 72a_1a_3a_5 \tag{80}$$

The discriminant Δ can be obtained from $\Delta_1^2 - 4\Delta_0^3 = -27\Delta$. The equation (75) has two distinct real roots and two complex conjugate non-real roots when $\Delta < 0$. The square root of the positive real root gives the optimal frequency where the harvested power is maximum.

The expression in equation (77) is exact but requires several calculations and not physically intuitive. From the equation of motion (66) we conjecture that the maximum power occurs around $\Omega^2 \approx \frac{\Gamma_k}{\Gamma_m}$. Using this, together with the small damping assumption, we can obtain a first-order approximation of the optimal frequency point as

$$\Omega_{\max}^2 \approx \frac{\Gamma_k}{\Gamma_m}\left[1 - \frac{\alpha^2\kappa^2\left(\left(1/2\,\kappa^2 - \Gamma_k\right)\beta + \Gamma_m\right)\beta}{\left(\left(\kappa^4 - 4\Gamma_k\kappa^2 + {\Gamma_k}^2\right)\alpha^2 + \Gamma_m\Gamma_k\right)\beta^2 - 2\Gamma_m\alpha^2\left(-\kappa^2 + \Gamma_k\right)\beta + {\Gamma_m}^2\alpha^2}\right] \tag{81}$$

The non-dimensional frequency for the maximum harvested power is therefore a function of the inertial amplifier parameters, time constant, normalised inductor parameter and the electromechanical coupling coefficient.

In Figure 12 the non-dimensional power is shown for two different inertial amplifiers. Five values of the damping

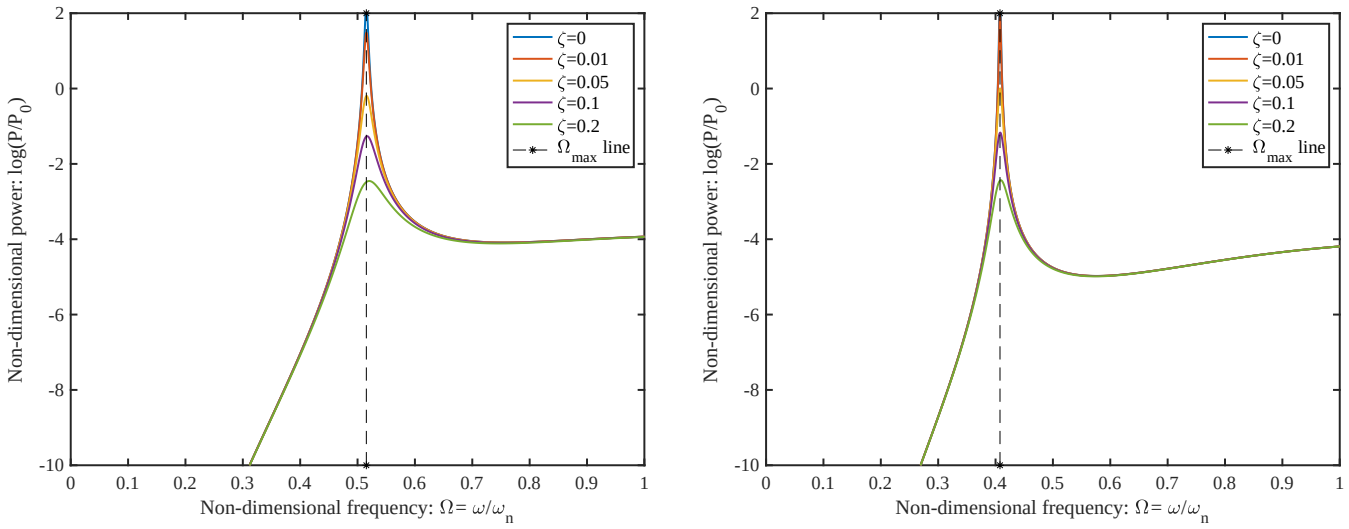

(a) Inertial amplifier with $\gamma_m = 0.2$, $\gamma_k = 1$, $\phi = 10°$

(b) Inertial amplifier with $\gamma_m = 1$, $\gamma_k = 0.6$, $\phi = 15°$

Figure 12. The non-dimensional power of a harvester with an inductor ($\alpha = 0.8649$, $\kappa^2 = 0.1185$, $\beta = 1.0$) as a function of the non-dimensional frequency for five selected values of damping factors. The value of the frequency of maximum power ($\Omega_{\max}$) obtained from equation (81) is shown in Figure 6 by a '*'. Five values of the damping factors of the energy harvesters have been considered for illustration.

factors of energy harvesters have been considered. They range from undamped to a damping factor of 20%. As expected, less damping in the harvester leads to more harvested power from the harmonic base excitation. The value of $\Omega_{\max}$ obtained from equation (81) is shown in Figure 12 by a '*'. It can be observed that it closely matches with the flow velocity for which the harvested power is maximum for all the five damping values. The non-dimensional frequency for the maximum power obtained from (81) are respectively 0.5154 and 0.4078. Note that for both the cases, this is significantly lower than the classical harvester without an inertial amplifier, for which $\Omega_{\max}$ is close to 1.

To gain further understanding on how the parameters of the inertial amplifier impact the frequency for the maximum power, in Figure 13 we show the contour lines of $\Omega_{\max}$ as functions of the stiffness ratio γ_k and inertial amplifier angle ϕ. Four values of the mass ratio γ_m and a damping factor of $\zeta = 0.011$ have been used. We also show the contour line of the frequency for the maximum power for the classical energy harvester without the inertial amplifier in the same plots. This is close to 1 and therefore any contour lines below this value show the parameter combinations for

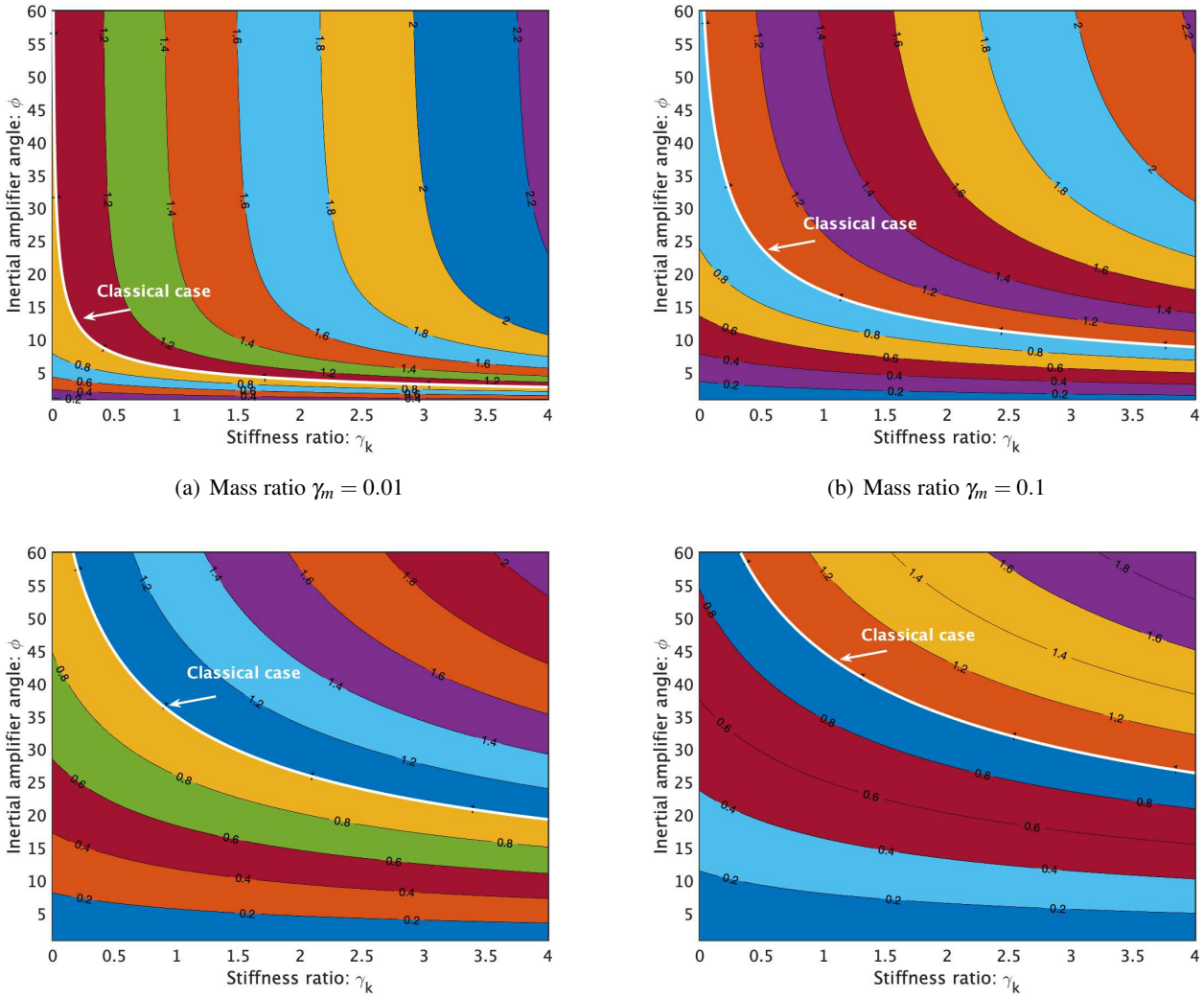

(a) Mass ratio $\gamma_m = 0.01$

(b) Mass ratio $\gamma_m = 0.1$

(c) Mass ratio $\gamma_m = 0.5$

(d) Mass ratio $\gamma_m = 1.0$

Figure 13. Contours of non-dimensional frequency for maximum power of a harvester with an inductor ($\zeta = 0.011$, $\alpha = 0.8649$, $\kappa^2 = 0.1185$, $\beta = 1.0$) as a function of the stiffness ratio γ_k and inertial amplifier angle ϕ. The non-dimensional frequency for maximum power for the equivalent classical harvester without an inertial amplifier is a constant (function of the electrical parameters only) and shown by a line as indicated. Contour lines below the classical line indicate that the maximum power of a harvester with an inertial amplifier takes place at a lower frequency. Higher values of the mass ratio γ_m and smaller amplifier angles ($\phi \lessapprox 15^\circ$) ensure this fact for any stiffness ratio.

which maximum power occurs below the classical case. A key observation is that for larger inertial amplifier mass (i.e., larger γ_m), a wider angle ϕ can be used to achieve a lower maximum frequency vale. For lower values of ϕ, $\Omega_{\max}$ is not very sensitive with γ_k.

The non-dimensional maximum harvested power is shown in Figure 14 as a function of the stiffness ratio γ_k and inertial amplifier angle ϕ for four different values of the mass ratio. The maximum power is obtained by computing the power at frequency values shown in Figure 12. We also show the contour line of the maximum power for the classical

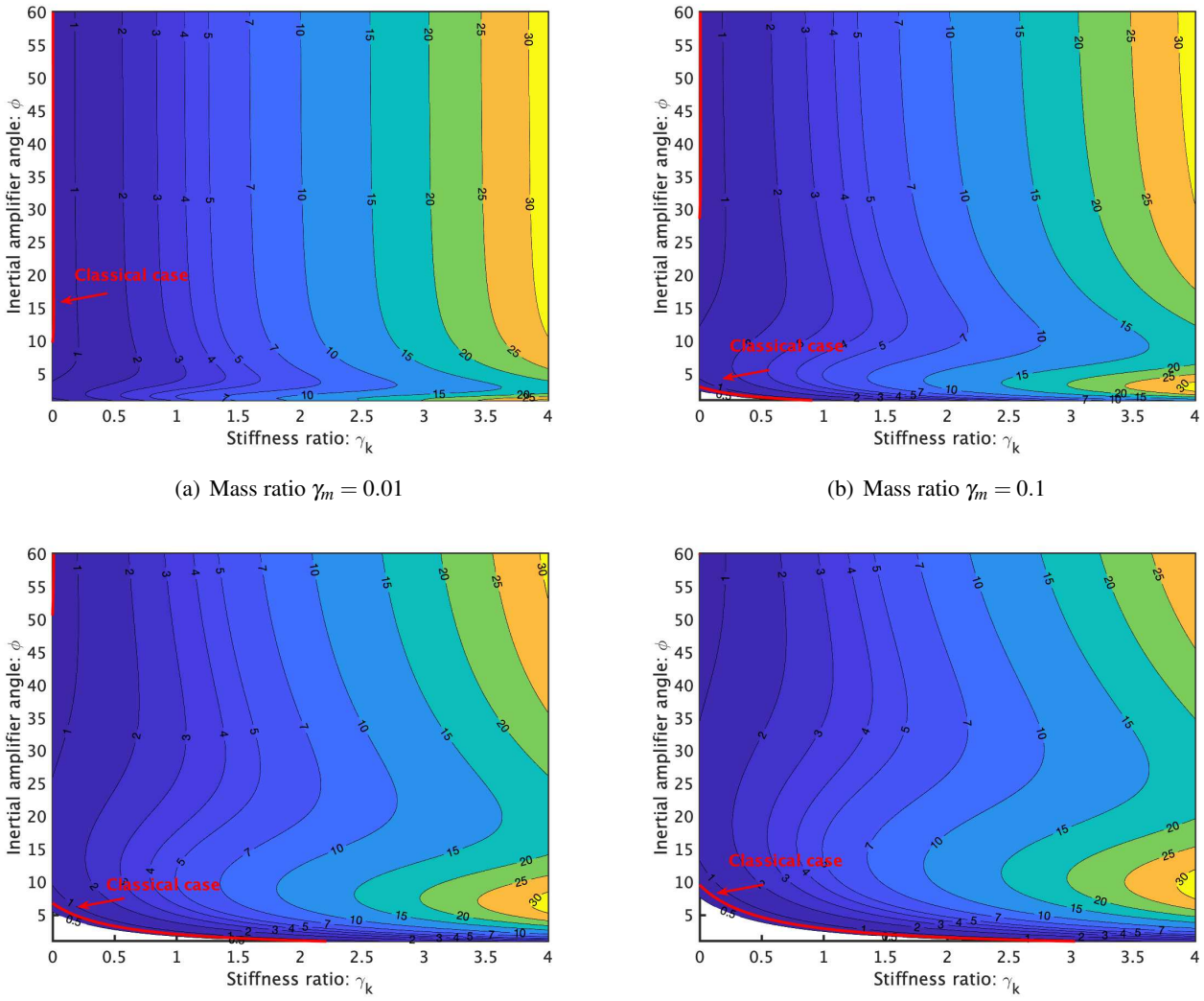

(a) Mass ratio $\gamma_m = 0.01$

(b) Mass ratio $\gamma_m = 0.1$

(c) Mass ratio $\gamma_m = 0.5$

(d) Mass ratio $\gamma_m = 1.0$

Figure 14. Contours of non-dimensional maximum power of a harvester with an inductor ($\zeta = 0.011$, $\alpha = 0.8649$, $\kappa^2 = 0.1185$, $\beta = 1.0$) as a function of the stiffness ratio γ_k and inertial amplifier angle ϕ. he non-dimensional maximum power for the equivalent classical harvester without an inertial amplifier is a constant (slightly more than 1) and shown by the indicated line. Contour lines above the classical line indicate that the maximum power of a harvester with an inertial amplifier is higher for the respective parameter combinations. Higher stiffness ratio γ_k leads to higher harvested power. However, the harvested power does not change significantly for larger amplifier angles, $\phi \gtrapprox 30^\circ$. Except for very small values of the stiffness ratio γ_k, maximum power obtained from the proposed harvester is always more than the classical harvester.

energy harvester without the inertial amplifier in the same plots. For most parameter combinations, the harvested power for the proposed system with inertial amplifier is more than the classical harvester. Increasing the stiffness in general leads to higher harvested power. We also observe that the harvested power does no change significantly beyond the inertial amplifier angle of 30°.

Form Figure 14 observe that a higher stiffness ratio generally γ_k leads to a higher harvested power for all values of

γ_m. However, Figure 14 shows that higher stiffness ratio γ_k leads to higher values of the frequency for the maximum power for the corresponding values of γ_m. This is not ideal for low-frequency energy harvesting. Therefore, the parameters should be selected for an optimal balance between maximum power and minimum frequency. Equation (81) along with figures 13 and 14 can give a practical approach towards selecting optimal parameters. As in the previous case, we select $\eta < 1$ as the desired normalised frequency value for the maximum harvested power. One can equate this quantity to the exact expression of the maximum frequency in (77). However, to simplify the analytical expression, the approximate expression in equation (81) has been used to obtain

$$\Gamma_m \eta^2 - \Gamma_k \left[1 - \frac{\alpha^2 \kappa^2 \left(\left(1/2\, \kappa^2 - \Gamma_k \right) \beta + \Gamma_m \right) \beta}{\left(\left(\kappa^4 - 4 \Gamma_k \kappa^2 + {\Gamma_k}^2 \right) \alpha^2 + \Gamma_m \Gamma_k \right) \beta^2 - 2 \Gamma_m \alpha^2 \left(-\kappa^2 + \Gamma_k \right) \beta + {\Gamma_m}^2 \alpha^2} \right] = 0 \tag{82}$$

Simplifying this equation we obtain

$$a_1 \Gamma_k^3 + a_2 \Gamma_k^2 + a_3 \Gamma_k + a_4 = 0 \tag{83}$$

where

$$\begin{aligned} a_1 &= 2\alpha^2\beta^2, a_2 = \left(\left(-2\beta^2\eta^2 - 4\beta \right) \alpha^2 + 2\beta^2 \right) \Gamma_m - 6\alpha^2\beta^2\kappa^2 \\ a_3 &= \left(\left(4\beta\,\eta^2 + 2 \right) \alpha^2 - 2\beta^2\eta^2 \right) {\Gamma_m}^2 + \left(8\beta^2\eta^2\,\kappa^2 + 2\beta\,\kappa^2 \right) \alpha^2 \Gamma_m + \alpha^2\beta^2\kappa^4 \\ \text{and} \quad a_4 &= -2\Gamma_m \alpha^2 \beta^2 \eta^2\, \kappa^4 - 4{\Gamma_m}^2 \alpha^2 \beta\, \eta^2\, \kappa^2 - 2{\Gamma_m}^3 \alpha^2 \eta^2 \end{aligned} \tag{84}$$

Equation (83) is a cubic equation in Γ_k and taking the real positive solution, the optimal value of the stiffness ratio can be obtained by using the expression of the cubic root given in (55). Using this, given a target frequency for the maximum power $\eta < 1$, one can explicitly choose the stiffness ratio given the parameters of the harvesting circuit and inertial amplifier parameters such as γ_k and ϕ. In Figure 15 we show the contours of the optimal non-dimensional stiffness ratio γ_k from equation (83) for different values of the inertial amplifier angle ϕ and target frequency for maximum power η. Results for four different values of the mass ratio are shown in Figure 15. When the mass ratio γ_m is small, say $\gamma_m = 0.01$ (that is only 1% of the tip mass), then it is not possible to obtain a real and positive value of the spring stiffness for a large number of parameter combinations as shown by the empty region in Figure 15(a). For larger inertial amplifier mass, more parameter combinations give physically realistic value of the spring stiffness for a target frequency for maximum power harvesting as seen in Figure 15(d). From these plots we also observe that if the inertial amplifier stiffness value to be kept low and a lower frequency for maximum power harvesting is needed, the mass of the inertial amplifier should be higher.

If the stiffness of the inertial amplifier is known or has been selected, then equation (59) can also be used to obtain γ_m and ϕ for maximum power at a prescribed target frequency value η. Equation (59) can be expressed in terms of a cubic polynomial in Γ_m as

$$a_1 \Gamma_m^3 + a_2 \Gamma_m^2 + a_3 \Gamma_m + a_4 = 0 \tag{85}$$

with coefficients

$$\begin{aligned} a_1 &= -2\,\eta^2\,\alpha^2, a_2 = \left(\left(4\beta\,\eta^2 + 2 \right) \alpha^2 - 2\beta^2\eta^2 \right) \Gamma_k - 4\beta\,\eta^2\,\kappa^2\alpha^2 \\ a_3 &= \left(\left(-2\beta^2\eta^2 - 4\beta \right) \alpha^2 + 2\beta^2 \right) {\Gamma_k}^2 + \left(8\beta^2\eta^2\,\kappa^2 + 2\beta\,\kappa^2 \right) \alpha^2 \Gamma_k - 2\beta^2\eta^2\,\kappa^4\alpha^2 \\ \text{and} \quad a_4 &= \Gamma_k \alpha^2\beta^2\kappa^4 - 6{\Gamma_k}^2\alpha^2\beta^2\kappa^2 + 2{\Gamma_k}^3\alpha^2\beta^2 \end{aligned} \tag{86}$$

The consideration of the real and positive root of the cubic equation (85) allows one to choose the optimal combination of γ_m and ϕ for the maximum power at frequency η. Next, we consider the case when the base excitation is a broadband random excitation.

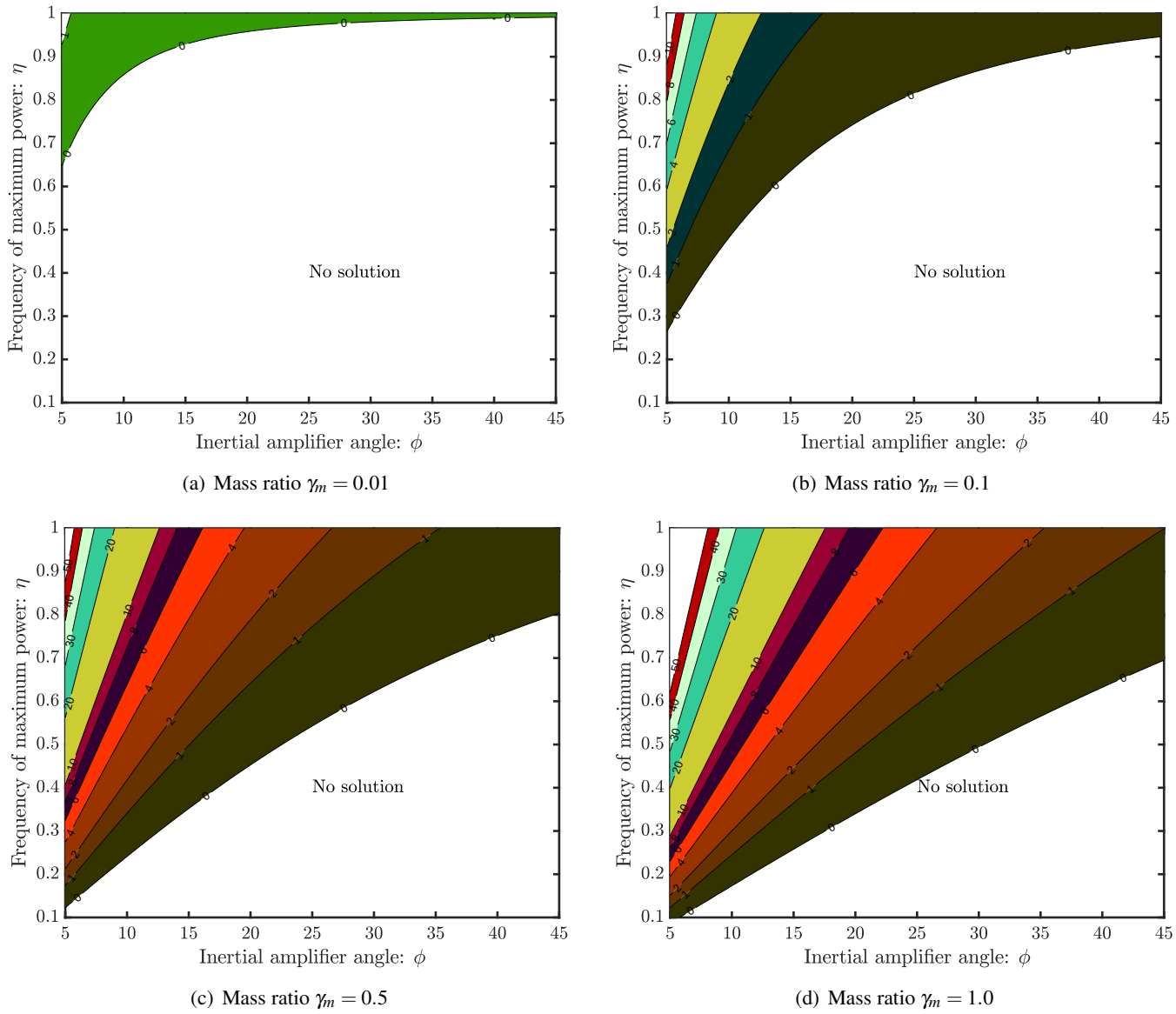

(a) Mass ratio $\gamma_m = 0.01$

(b) Mass ratio $\gamma_m = 0.1$

(c) Mass ratio $\gamma_m = 0.5$

(d) Mass ratio $\gamma_m = 1.0$

Figure 15. Contours of the optimal non-dimensional stiffness stiffness ratio γ_k for of a harvester with an inductor ($\zeta = 0.011$, $\alpha = 0.8649$, $\kappa^2 = 0.1185$, $\beta = 1.0$) as a function of the target frequency for the maximum power η and inertial amplifier angle ϕ. The empty region marked above show the parameter combination when t is not possible to obtain a real and positive value of the stiffness ratio.

4 Energy harvesting from broadband random base excitation

It is considered that the base excitation $y_b(t)$ is a broadband, Gaussian and weakly stationary random process. Dynamical systems subjected to this type of excitation have been discussed by Lin [11], Nigam [12], Bolotin [13], Roberts and Spanos [14] and Newland [15] using the theory of random vibration . In Figure 16 illustrations of a white noise base excitation and a harmonic base excitation are shown.

We are interested in the average harvested power given by

$$\mathrm{E}[P(t)] = \mathrm{E}\left[\frac{v^2(t)}{R_l}\right] = \frac{\mathrm{E}\left[v^2(t)\right]}{R_l} \tag{87}$$

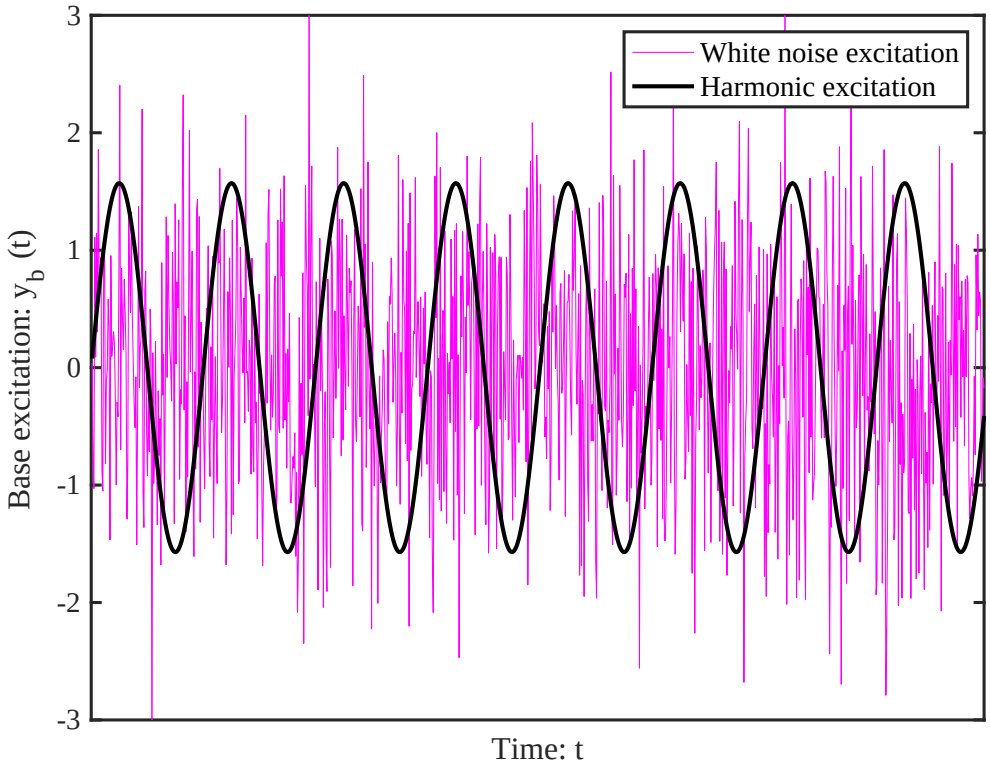

Figure 16. Illustrations of a white noise base excitation and a harmonic base excitation. We consider that the base excitation $y_b(t)$ is a weakly stationary, Gaussian, broadband random process. The strength of the white noise shown here is considered to be 1 as an example. The harvested power is quantified due to both types of input excitations.

For a damped linear system of the form $V(\omega) = H(\omega)Y_b(\omega)$, it can be shown that [11, 12] the spectral density of the voltage V is related to the spectral density of the base excitation Y_b (denoted by $\Phi_{y_b y_b}(\omega)$) through

$$\Phi_{VV}(\omega) = |H(\omega)|^2 \Phi_{y_b y_b}(\omega) \tag{88}$$

Thus, for large t, we obtain

$$\mathrm{E}\left[v^2(t)\right] = R_{vv}(0) = \int_{-\infty}^{\infty} |H(\omega)|^2 \Phi_{y_b y_b}(\omega)\, \mathrm{d}\omega \tag{89}$$

This expression will be used to obtain the average power for the two cases considered. We assume that the base acceleration $\ddot{y}_b(t)$ is a Gaussian white noise so that its spectral density is constant with respect to frequency.

4.1 Circuit without an inductor

The schematic diagram of a cantilever piezoelectric energy harvester for this case shown in Figure 4. We derive mathematical expressions for the mean harvested power and obtain the parameter combinations which maximise it.

4.1.1 Quantification of the mean harvested power

From equation (48) we obtain the voltage in the frequency domain as

$$V = \frac{-\mathrm{i}\Omega^3 \frac{\alpha\theta}{C_p}\Gamma_m}{\Delta_1(\mathrm{i}\Omega)} Y_b \tag{90}$$

Following duToit and Wardle [7] and Adhkari et. al [8] we are interested in the mean of the normalised harvested power when the base acceleration is Gaussian white noise, that is $|V|^2/(R_l\omega^4\Phi_{y_by_b})$. Note that $\Phi_{y_by_b})$ is the spectral density of the acceleration and is assumed to be constant. After some algebra, from equation (90), the normalized power is

$$\widetilde{P} = \frac{|V|^2}{(R_l\omega^4\Phi_{y_by_b})} = \frac{k\alpha\kappa^2\Gamma_m^2}{\omega_n^3}\frac{\Omega^2}{\Delta_1(\mathrm{i}\Omega)\Delta_1^*(\mathrm{i}\Omega)}. \tag{91}$$

Using equation (89), the average normalized power can be obtained as

$$\mathrm{E}\left[\widetilde{P}\right] = \mathrm{E}\left[\frac{|V|^2}{(R_l\omega^4\Phi_{y_by_b})}\right] = \frac{k\alpha\kappa^2\Gamma_m^2}{\omega_n^3}\int_{-\infty}^{\infty}\frac{\Omega^2}{\Delta_1(\mathrm{i}\Omega)\Delta_1^*(\mathrm{i}\Omega)}\,\mathrm{d}\omega \tag{92}$$

From equation (45) observe that $\Delta_1(\mathrm{i}\Omega)$ is a third-order polynomial in $(\mathrm{i}\Omega)$. Noting that $\mathrm{d}\omega = \omega_n\mathrm{d}\Omega$ and from equation (45), the average harvested power can be obtained from equation (92) as

$$\mathrm{E}\left[\widetilde{P}\right] = \mathrm{E}\left[\frac{|V|^2}{(R_l\omega^4\Phi_{y_by_b})}\right] = m\alpha\kappa^2\Gamma_m^2\underbrace{\int_{-\infty}^{\infty}\frac{\Omega^2}{\Delta_1(\mathrm{i}\Omega)\Delta_1^*(\mathrm{i}\Omega)}\mathrm{d}\Omega}_{I^{(1)}} \tag{93}$$

The calculation of the integral of the form $I^{(1)}$ on the right-hand side of equation (93) in general requires the calculation of integrals of the following type

$$I_n = \int_{-\infty}^{\infty}\frac{\Xi_n(\omega)\,\mathrm{d}\omega}{\Lambda_n(\omega)\Lambda_n^*(\omega)} \tag{94}$$

where the polynomials have the form

$$\Xi_n(\omega) = b_{n-1}\omega^{2n-2} + b_{n-2}\omega^{2n-4} + \cdots + b_0 \tag{95}$$

$$\Lambda_n(\omega) = a_n(\mathrm{i}\omega)^n + a_{n-1}(\mathrm{i}\omega)^{n-1} + \cdots + a_0 \tag{96}$$

Following Roberts and Spanos [14] this integral can be evaluated as

$$I_n = \frac{\pi}{a_n}\frac{\det[\mathbf{D}_n]}{\det[\mathbf{N}_n]} \tag{97}$$

Here the $n \times n$ matrices are defined as

$$\mathbf{D}_n = \begin{bmatrix} b_{n-1} & b_{n-2} & & \cdots & & & b_0 \\ -a_n & a_{n-2} & -a_{n-4} & a_{n-6} & \cdots & 0 & \cdots \\ 0 & -a_{n-1} & a_{n-3} & -a_{n-5} & \cdots & 0 & \cdots \\ 0 & a_n & -a_{n-2} & a_{n-4} & \cdots & 0 & \cdots \\ 0 & \cdots & & & \cdots & 0 & \cdots \\ 0 & 0 & & & \cdots & -a_2 & a_0 \end{bmatrix} \tag{98}$$

and

$$\mathbf{N}_n = \begin{bmatrix} a_{n-1} & -a_{n-3} & a_{n-5} & -a_{n-7} & & & \\ -a_n & a_{n-2} & -a_{n-4} & a_{n-6} & \cdots & 0 & \cdots \\ 0 & -a_{n-1} & a_{n-3} & -a_{n-5} & \cdots & 0 & \cdots \\ 0 & a_n & -a_{n-2} & a_{n-4} & \cdots & 0 & \cdots \\ 0 & \cdots & & & \cdots & 0 & \cdots \\ 0 & 0 & & & \cdots & -a_2 & a_0 \end{bmatrix}. \tag{99}$$

Comparing $I^{(1)}$ with the general integral in equation (94) we have

$$\begin{aligned} & n=3, b_2=0, b_1=1, b_0=0 \\ \text{and} \quad & a_3=\alpha\Gamma_m, a_2=\left(2\zeta\,\alpha+\Gamma_m\right), a_1=\left(\kappa^2+\Gamma_k\right)\alpha+2\zeta, a_0=\Gamma_k \end{aligned} \tag{100}$$

Now using equation (97), the integral can be evaluated as

$$I^{(1)}=\frac{\pi}{\alpha\Gamma_m}\frac{\det\begin{bmatrix} 0 & 1 & 0 \\ -\Gamma_m\alpha & \left(\kappa^2+\Gamma_k\right)\alpha+2\zeta & 0 \\ 0 & -2\alpha\zeta-\Gamma_m & \Gamma_k \end{bmatrix}}{\det\begin{bmatrix} 0 & 1 & 0 \\ -\Gamma_m\alpha & \left(\kappa^2+\Gamma_k\right)\alpha+2\zeta & 0 \\ 0 & -2\alpha\zeta-\Gamma_m & \Gamma_k \end{bmatrix}}=\frac{\pi}{2\zeta\left(\kappa^2+\Gamma_k\right)\alpha^2+\left(\Gamma_m\kappa^2+4\zeta^2\right)\alpha+2\Gamma_m\zeta} \tag{101}$$

Combining this with equation (92) we finally obtain the average harvested power due to the white-noise base acceleration as

$$\mathrm{E}\left[\widetilde{P}\right]=\left(m\alpha\kappa^2\Gamma_m^2\right)I^{(1)}=\frac{\pi m\alpha\kappa^2\Gamma_m^2}{2\zeta\left(\kappa^2+\Gamma_k\right)\alpha^2+\left(\Gamma_m\kappa^2+4\zeta^2\right)\alpha+2\Gamma_m\zeta} \tag{102}$$

To gain further understanding on how the parameters of the inertial amplifier impact the mean harvested power due to a random broadband base excitation, in Figure 17 we show the contour lines of the normalised mean power ratio as functions of the stiffness ratio γ_k and inertial amplifier angle ϕ. The normalised mean power ratio is calculated by dividing the power obtained from equation (102) with the equivalent power from a classical harvester. This can be obtained by substituting $\Gamma_k=\Gamma_m=1$ is equation (102) as

$$\mathrm{E}\left[\widetilde{P}\right]_{\text{classical}}=\frac{\pi m\alpha\kappa^2}{2\zeta\left(\kappa^2+1\right)\alpha^2+\left(\kappa^2+4\zeta^2\right)\alpha+2\zeta} \tag{103}$$

Four values of the mass ratio, namely $\gamma_m=0.01,0.1.0.2,0.5.$ and a damping factor of $\zeta=0.011$ have been used. All other parameters are as given in Table 1. As this plot is the ratio of the power with respect to the classical energy harvester, all contour lines above 1 demonstrate the enhanced harvested power with the inertial amplifier. In general more power is harvested with smaller inertial amplifier angle ϕ. A key observation is that the normalised mean power ratio is not very sensitive with the stiffness ratio γ_k.

4.1.2 Optimisation of the mean harvested power

We aim to derive physically realistic parameter combination which will maximise the mean harvested power as given by equation (102). Maximizing the average power with respect to α gives the condition

$$\alpha^2\left(\Gamma_k+\kappa^2\right)=\Gamma_m \tag{104}$$

In terms of the physical quantities, the optimal condition can be expressed as

$$R_l^2C_p\left(\left(k+k_a\right)C_p+\theta^2\right)=m+m_a\cot^2\phi \tag{105}$$

If the circuit parameters are fixed, from equation (104) one can determine the design spring ratio as

$$\gamma_k=\frac{1+\gamma_m\cot^2\phi}{\alpha^2}-\left(1+\kappa^2\right) \tag{106}$$

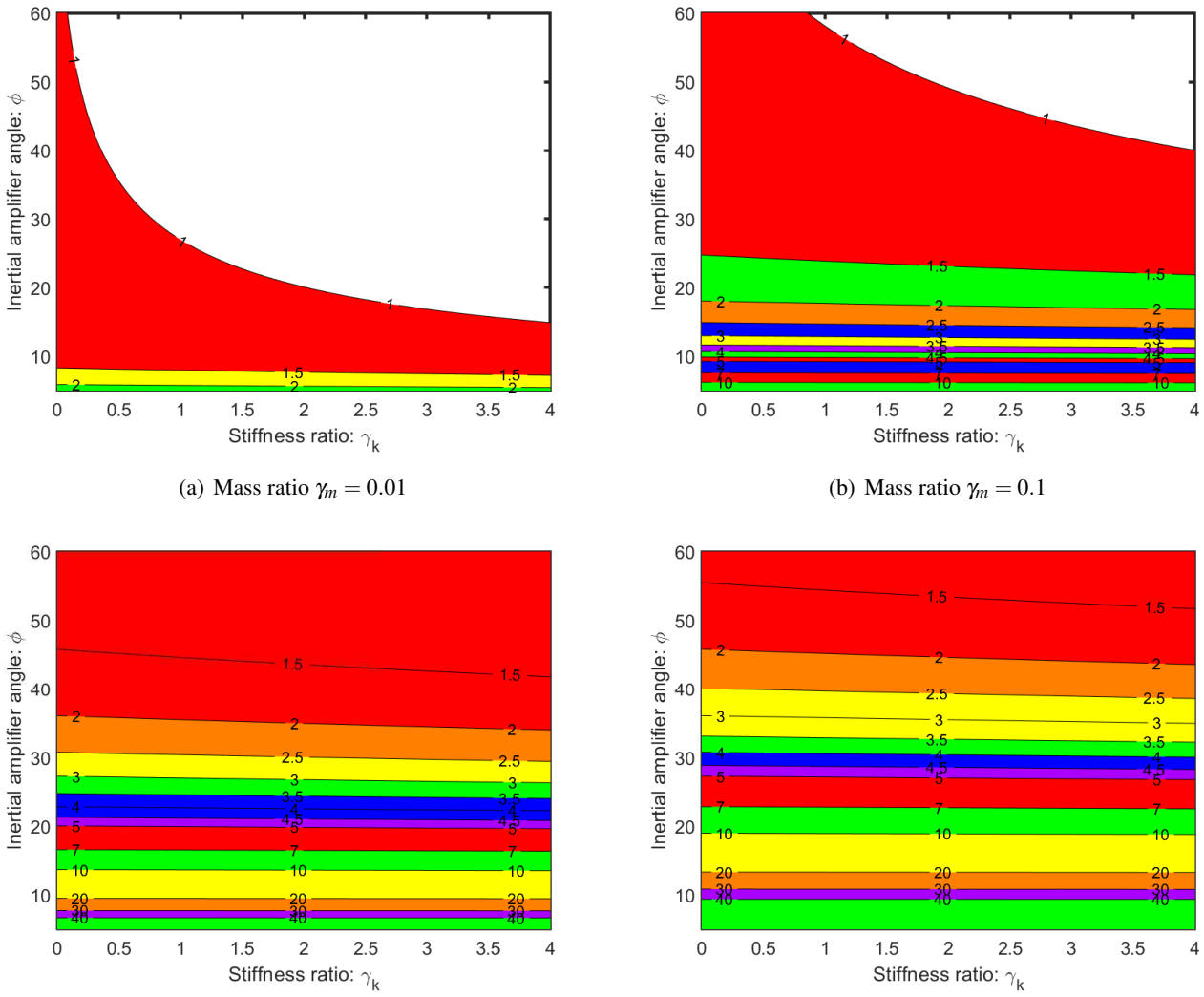

(a) Mass ratio $\gamma_m = 0.01$

(b) Mass ratio $\gamma_m = 0.1$

(c) Mass ratio $\gamma_m = 0.5$

(d) Mass ratio $\gamma_m = 1.0$

Figure 17. Normalised mean power ratio ($\mathrm{E}\left[\widetilde{P}\right]/\mathrm{E}\left[\widetilde{P}\right]_{\text{classical}}$) of a harvester without an inductor ($\zeta = 0.011$, $\alpha = 0.8649$, $\kappa^2 = 0.1185$) as a function of the stiffness ratio γ_k and inertial amplifier angle ϕ. For $\phi \lessapprox 20°$, the mean harvested power ratio does not change significantly with γ_k. As this plot is the ratio of the power with respect to the classical energy harvester, all contour lines above 1 demonstrate the enhanced harvested power with the inertial amplifier. Lower values of the inertial amplifier angle ϕ leads to significantly higher power even for smaller values of the stiffness ratio γ_k.For higher value of the mass ratio γ_m, more power is harvested irrespective of other parameter values.

Using the relationship in (104) in the expression of the mean harvested power in (102), we obtain the maximum power as

$$\mathrm{E}\left[\widetilde{P}\right]_{\max} = \frac{\pi m \alpha\, \kappa^2 \Gamma_m^2}{(\alpha\,\kappa^2 + 4\,\zeta)\,\Gamma_m + 4\,\alpha\,\zeta^2} \tag{107}$$

The normalised mean power ratio as a function of α is shown in Figure 18 considering $\zeta = 0.1$ and $\kappa = 0.6$. The normalised mean power ratio is obtained by diving the mean power of the harvester with the inertial amplifier with the mean power of the classical harvester with the optimal α given by (104). Four values of γ_m and ϕ are used in the

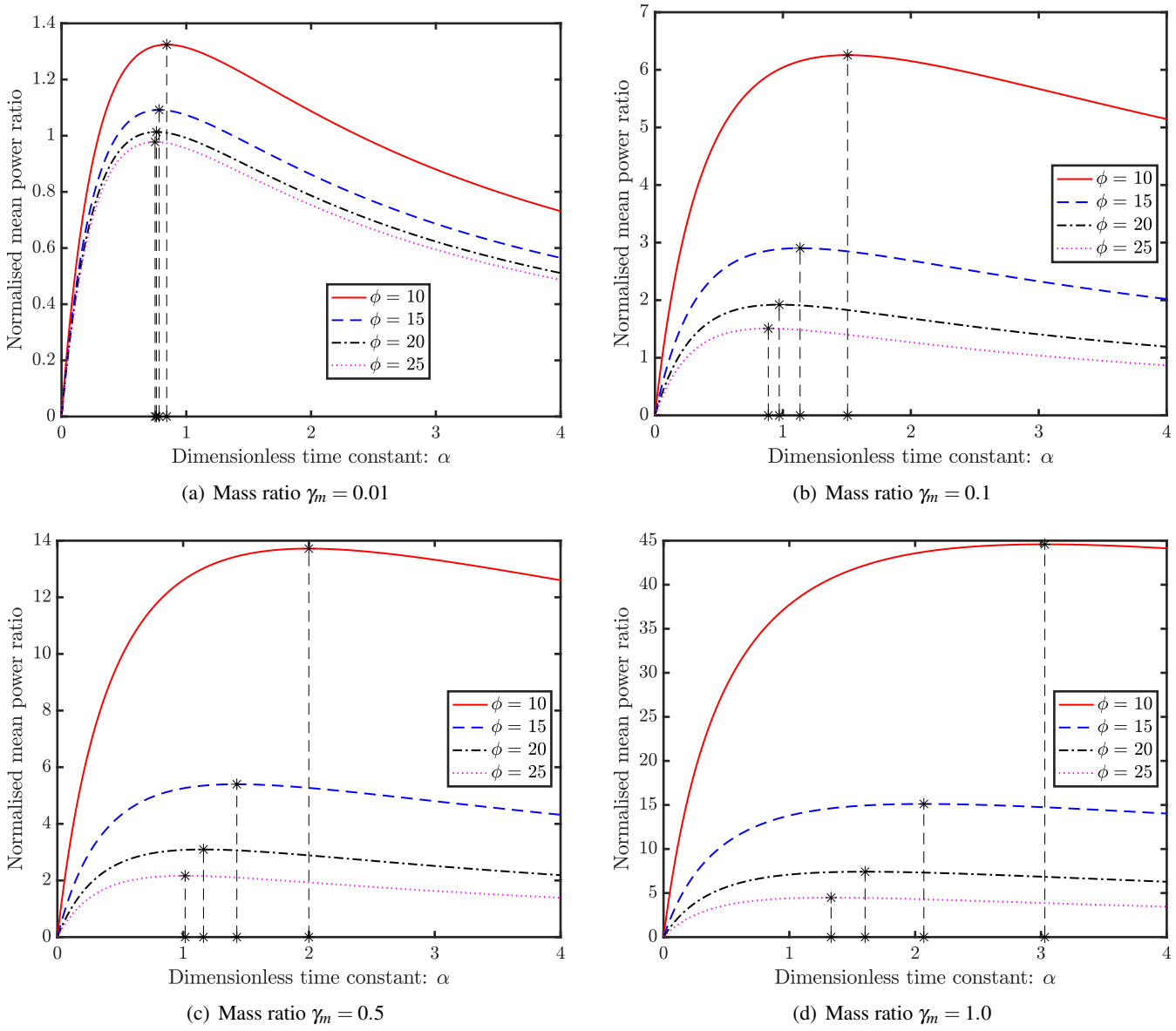

(a) Mass ratio $\gamma_m = 0.01$

(b) Mass ratio $\gamma_m = 0.1$

(c) Mass ratio $\gamma_m = 0.5$

(d) Mass ratio $\gamma_m = 1.0$

Figure 18. The normalised mean power ratio of a harvester without an inductor as a function of α for $\zeta = 0.1$, $\gamma_k = 0.5$ and $\kappa = 0.6$. Four values of γ_m and ϕ are used in the plots. The * corresponds to the optimal values of α for the maximum mean harvested power obtained from equation (104).

plots along with $\zeta = 0.1$, $\gamma_k = 0.5$, and $\kappa = 0.6$. The optimal values of α obtained from equation (104) are marked in the figures. Figure 18 clearly confirms the accuracy of the maximum power obtained with the theoretically predicted optimal values. The amplification reduce for smaller values of the mass ratio and larger values of the inertial amplifier angle. When the mass ratio $\gamma_m = 1$ and the inertial amplifier angle $\phi = 10^\circ$, the mean power harvested form the proposed inertial amplifier based energy harvester can be 45 times more than the power harvested form the classical energy harvester as can be observed in Figure 18(d).

4.2 Circuit with an inductor

The schematic diagram of a cantilever piezoelectric energy harvester for this case shown in Figure 10. We derive mathematical expressions for the mean harvested power and obtain the parameter combinations which maximise it.

4.2.1 Quantification of the mean harvested power

For this case, from equation (70) we obtain the voltage in the frequency domain as

$$V = \frac{\Omega^4 \dfrac{\alpha\beta\theta\Gamma_m}{C_p}}{\Delta_2(\mathrm{i}\Omega)} Y_b \tag{108}$$

Following references [8, 10] the average normalized harvested power can be expressed as

$$\mathrm{E}\left[\widetilde{P}\right] = \mathrm{E}\left[\frac{|V|^2}{(R_l\omega^4\Phi_{y_b y_b})}\right] = m\alpha\beta^2\kappa^2\Gamma_m^2 \underbrace{\int_{-\infty}^{\infty} \frac{\Omega^4}{\Delta_2(\mathrm{i}\Omega)\Delta_2^*(\mathrm{i}\Omega)}\,\mathrm{d}\Omega}_{I^{(2)}} \tag{109}$$

Using the expression of $\Delta_2(\mathrm{i}\Omega)$ in equation (68) and comparing $I^{(2)}$ with the general integral in equation (94) we have

$$\begin{aligned} &n = 4, b_3 = 0, b_2 = 1, b_1 = 0, b_0 = 0, a_4 = \Gamma_m\beta\alpha, a_3 = \beta\left(2\zeta\,\alpha + \Gamma_m\right) \\ \text{and}\quad &a_2 = \left(\left(\kappa^2 + \Gamma_k\right)\beta + \Gamma_m\right)\alpha + 2\beta\,\zeta, a_1 = \left(\beta\Gamma_k + 2\zeta\,\alpha\right), a_0 = \alpha\Gamma_k \end{aligned} \tag{110}$$

Now using equation (97), the integral can be evaluated as

$$I^{(2)} = \frac{\pi}{\Gamma_m\beta\alpha} \frac{\det\begin{bmatrix} 0 & 1 & 0 & 0 \\ -\Gamma_m\alpha\beta & \left(\left(\kappa^2+\Gamma_k\right)\beta+\Gamma_m\right)\alpha+2\beta\,\zeta & -\Gamma_k\alpha & 0 \\ 0 & -\beta\left(2\alpha\,\zeta+\Gamma_m\right) & \Gamma_k\beta+2\alpha\,\zeta & 0 \\ 0 & -\Gamma_m\alpha\beta & \left(\left(\kappa^2+\Gamma_k\right)\beta+\Gamma_m\right)\alpha+2\beta\,\zeta & \Gamma_k\alpha \end{bmatrix}}{\det\begin{bmatrix} \beta\left(2\alpha\,\zeta+\Gamma_m\right) & -\Gamma_k\beta-2\alpha\,\zeta & 0 & 0 \\ -\Gamma_m\alpha\beta & \left(\left(\kappa^2+\Gamma_k\right)\beta+\Gamma_m\right)\alpha+2\beta\,\zeta & -\Gamma_k\alpha & 0 \\ 0 & -\beta\left(2\alpha\,\zeta+\Gamma_m\right) & \Gamma_k\beta+2\alpha\,\zeta & 0 \\ 0 & -\Gamma_m\alpha\beta & \left(\left(\kappa^2+\Gamma_k\right)\beta+\Gamma_m\right)\alpha+2\beta\,\zeta & \Gamma_k\alpha \end{bmatrix}} \tag{111}$$

Combining this with equation (109) we finally obtain the average normalized harvested power as

$$\begin{aligned} \mathrm{E}\left[\widetilde{P}\right] = \frac{m\alpha\,\beta\,\kappa^2{\Gamma_m}^2\pi\left(\Gamma_k\beta+2\alpha\,\zeta\right)}{&\left(\left(2\Gamma_k\alpha^2\zeta+\Gamma_m\Gamma_k\alpha\right)\kappa^2+4\Gamma_k\zeta^2\alpha+\left(2{\Gamma_k}^2\alpha^2+2\Gamma_m\Gamma_k\right)\zeta\right)\beta^2 \\ &+\left(\left(4\alpha^3\zeta^2+2\Gamma_m\alpha^2\zeta\right)\kappa^2-4\Gamma_m\Gamma_k\alpha^2\zeta+8\alpha^2\zeta^3+4\Gamma_m\alpha\,\zeta^2\right)\beta+2{\Gamma_m}^2\alpha^2\zeta \end{aligned} \tag{112}$$

This is the complete closed-form expression of the normalized harvested power under a Gaussian white noise base acceleration.

To gain further understanding on how the parameters of the inertial amplifier impact the mean harvested power due to random broadband base excitation, in Figure 19 we show the contour lines of the normalised mean power ratio as functions of the stiffness ratio γ_k and inertial amplifier angle ϕ. The normalised mean power ratio is calculated by

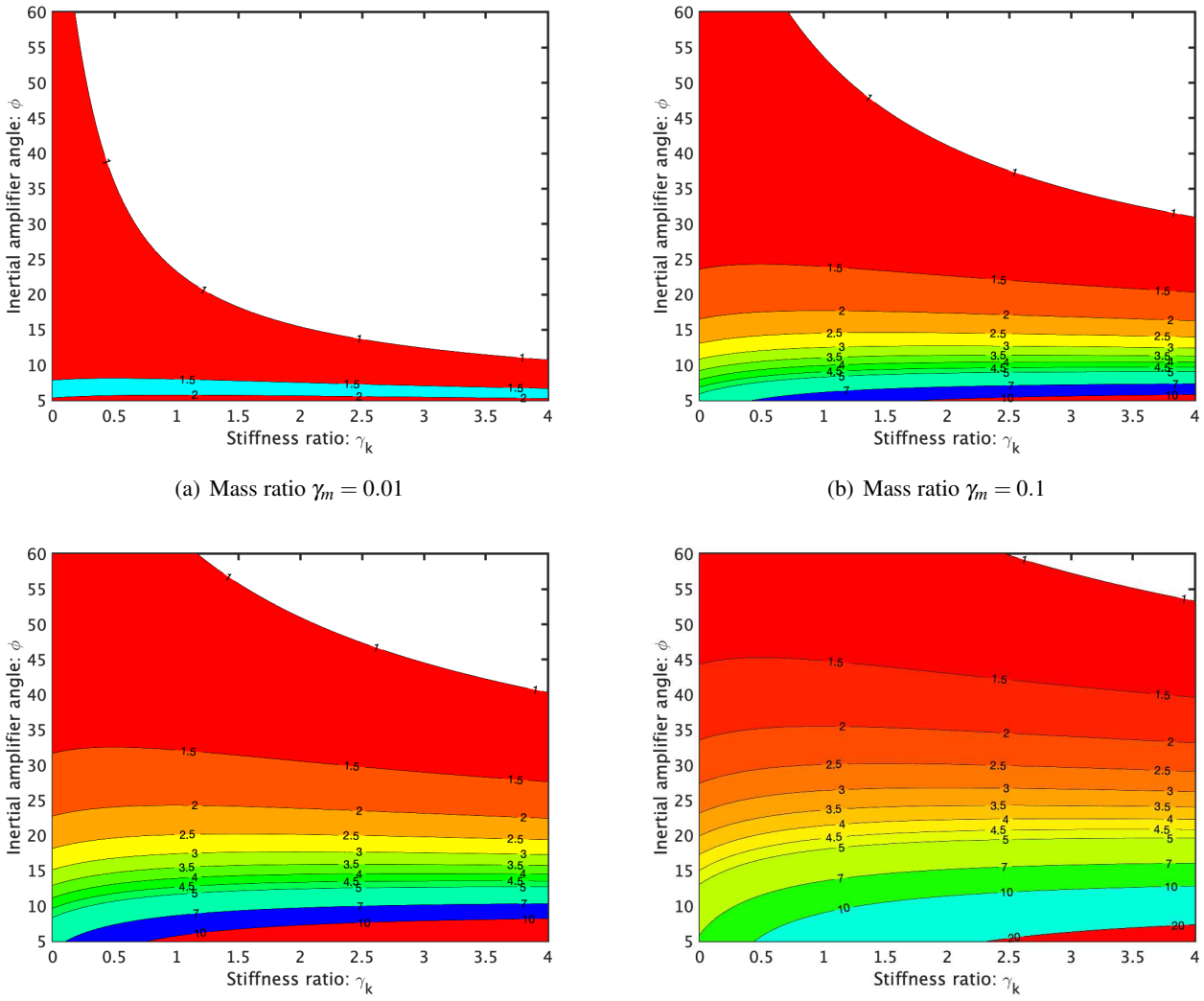

(a) Mass ratio $\gamma_m = 0.01$

(b) Mass ratio $\gamma_m = 0.1$

(c) Mass ratio $\gamma_m = 0.5$

(d) Mass ratio $\gamma_m = 1.0$

Figure 19. Normalised mean power ratio ($\mathrm{E}\left[\widetilde{P}\right]/\mathrm{E}\left[\widetilde{P}\right]_{\text{classical}}$) of a harvester with an inductor ($\zeta = 0.011$, $\alpha = 0.8649$, $\kappa^2 = 0.1185$, $\beta = 1.0$) as a function of the stiffness ratio γ_k and inertial amplifier angle ϕ. For $\phi \lessapprox 20^\circ$, the mean harvested power ratio does not change significantly with γ_k. As this plot is the ratio of the power with respect to the classical energy harvester, all contour lines above 1 demonstrate the enhanced harvested power with the inertial amplifier. Lower values of the inertial amplifier angle ϕ leads to significantly higher power even for smaller values of the stiffness ratio γ_k.For higher value of the mass ratio γ_m, more power is harvested irrespective of other parameter values.

dividing the power obtained from equation (112) with the equivalent power from a classical harvester. This can be obtained by substituting $\Gamma_k = \Gamma_m = 1$ is equation (112) as

$$\mathrm{E}\left[\widetilde{P}\right]_{\text{classical}} = \frac{m\alpha\beta\kappa^2\pi\left(\beta+2\alpha\zeta\right)}{\beta\left(\beta+2\alpha\zeta\right)\left(1+2\alpha\zeta\right)\left(\alpha\kappa^2+2\zeta\right)+2\alpha^2\zeta\left(\beta-1\right)^2} \tag{113}$$

Four values of the mass ratio, namely $\gamma_m = 0.01, 0.1 0.5, 1.0$. and a damping factor of $\zeta = 0.011$ have been used. All other parameters are as given in Table 1. As this plot is the ratio of the power with respect to the classical energy

harvester, all contour lines above 1 demonstrate the enhanced harvested power with the inertial amplifier. In general more power is harvested with smaller inertial amplifier angle ϕ and higher mass ratio γ_m. A key observation is that the normalised mean power ratio is not very sensitive with the stiffness ratio γ_k.

4.2.2 Optimisation of the mean harvested power

We aim to derive physically realistic parameter combination which will maximise the mean harvested power as given by equation (112). We can also determine optimum values for Γ_m and Γ_k. Setting the derivative of the mean power in (112) with respect to Γ_k to zero we have

$$\frac{\mathrm{d}\left(\mathrm{E}\left[\widetilde{P}\right]\right)}{\mathrm{d}\Gamma_k} = 0 \tag{114}$$

Considering the positive solution of the resulting equation, the optimal condition can be expressed as

$$\beta\Gamma_k = \Gamma_m \tag{115}$$

In terms of physical quantities the optimal condition can be expressed as

$$L_i C_p\,(k + k_a) = m + m_a \cot^2\phi \tag{116}$$

If the circuit parameters are fixed, from equation (115) one can determine the design spring ratio as

$$\gamma_k = \frac{1 + \gamma_m \cot^2\phi}{\beta^2} - 1 \tag{117}$$

Substituting optimal relationship from (115) in the expression of the mean harvested power in (112), we obtain the maximum power as

$$\mathrm{E}\left[\widetilde{P}\right]_{\mathrm{opt}} = \frac{m\pi {\Gamma_m}^2 \alpha\,\kappa^2}{(\kappa^2\alpha + 2\,\zeta)\,(2\,\alpha\,\zeta + \Gamma_m)} \tag{118}$$

It can be observed that this maximum value is independent of the stiffness ratio γ_k and the inductor parameter β. The normalised mean power ratio as a function of β is shown in Figure 20 considering $\alpha = 0.8649$, $\zeta = 0.1$ and $\kappa = 0.6$. The normalised mean power ratio is obtained by diving the mean power of the harvester with the inertial amplifier with the mean power of the classical harvester with the optimal β given by (115). Four values of γ_m and ϕ are used in the plots along with $\zeta = 0.1$, $\gamma_k = 0.5$, and $\kappa = 0.6$. The optimal values of β obtained from equation (115) are shown by a * in the figure. Figure 20 clearly demonstrates that the maximum power is obtained with the optimal value of β obtained from equation (115). The amplification in the harvested power reduce for smaller values of the mass ratio and larger values of the inertial amplifier angle. When the mass ratio $\gamma_m = 1$ and the inertial amplifier angle $\phi = 10^\circ$, the mean power harvested form the proposed inertial amplifier based energy harvester can be 45 times more than the power harvested form the classical energy harvester as can be observed in Figure 18(d).

If κ and ζ are fixed, then by further differentiating equation (118) with respect to α we obtain the optimal value as

$$\alpha = \frac{\sqrt{\Gamma_m}}{\kappa} \tag{119}$$

In terms of the physical quantities, the optimal condition can be expressed as

$$R_l^2 C_p \theta^2 = m + m_a \cot^2\phi \tag{120}$$

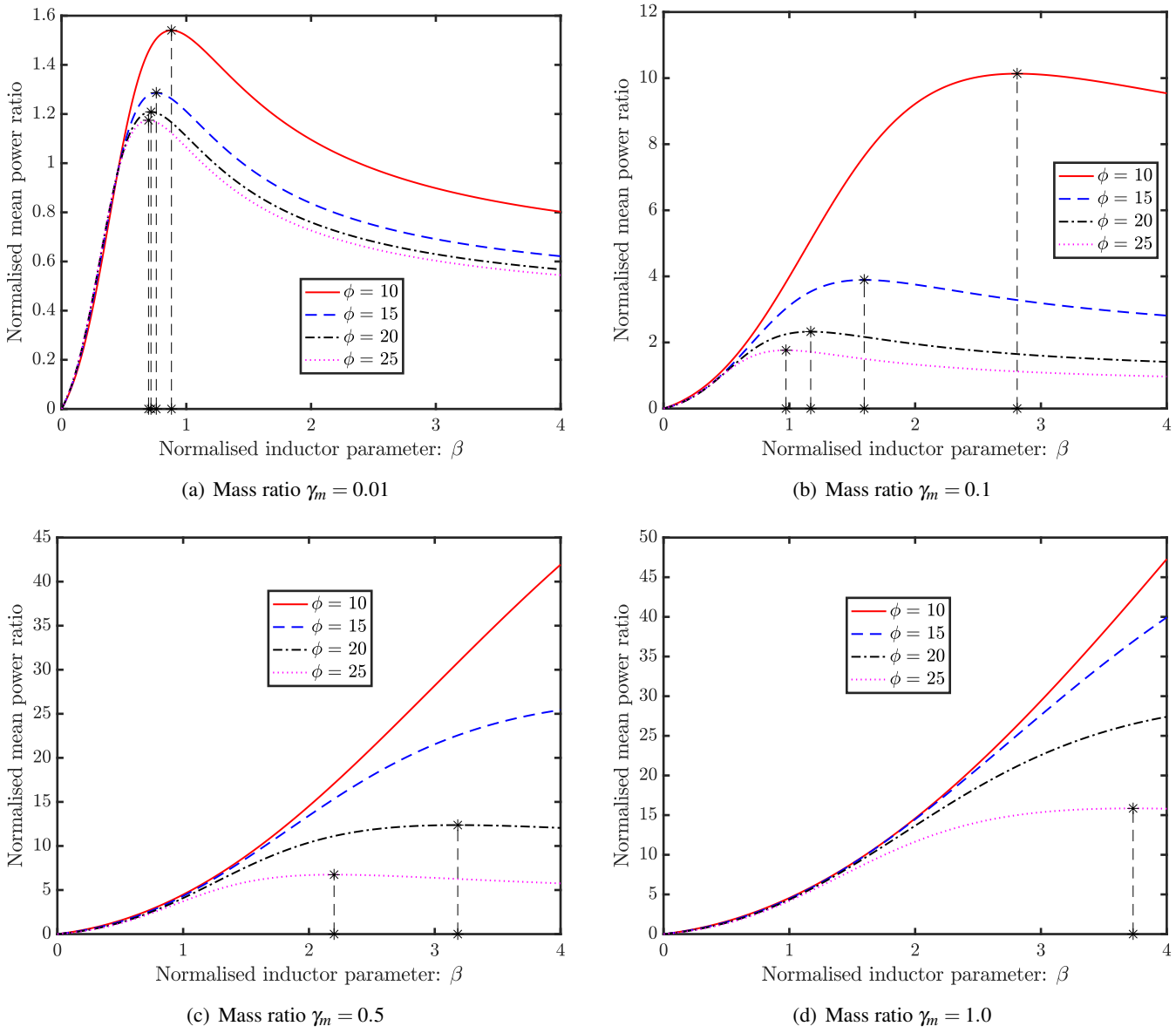

(a) Mass ratio $\gamma_m = 0.01$

(b) Mass ratio $\gamma_m = 0.1$

(c) Mass ratio $\gamma_m = 0.5$

(d) Mass ratio $\gamma_m = 1.0$

Figure 20. The normalised mean power ratio of a harvester with an inductor as a function of β for $\alpha = 0.8649$, $\zeta = 0.1$, $\gamma_k = 0.5$ and $\kappa = 0.6$. The * corresponds to the optimal value of β for the maximum mean harvested power obtained from equation (115).

With this choice, the absolute maxima of the mean harvested power is obtained as

$$\mathrm{E}\left[\widetilde{P}\right]_{\max} = \frac{m\pi{\Gamma_m}^2\kappa^2}{\left(\sqrt{\Gamma_m}\kappa + 2\zeta\right)^2} \tag{121}$$

The normalised mean power ratio as a function of α is shown in Figure 21 considering $\zeta = 0.1$ and $\kappa = 0.6$. The normalised mean power ratio is obtained by diving the mean power of the harvester with the inertial amplifier with the mean power of the classical harvester with the optimal β and α given by equations (115) and (119). The parameters for the energy harvester are considered as $\zeta = 0.1$, $\gamma_k = 0.5$ and $\kappa = 0.6$ as before. The optimal values of α obtained from equation (119) are marked by *. Figure 21 clearly demonstrates the maximum power obtained with the optimal

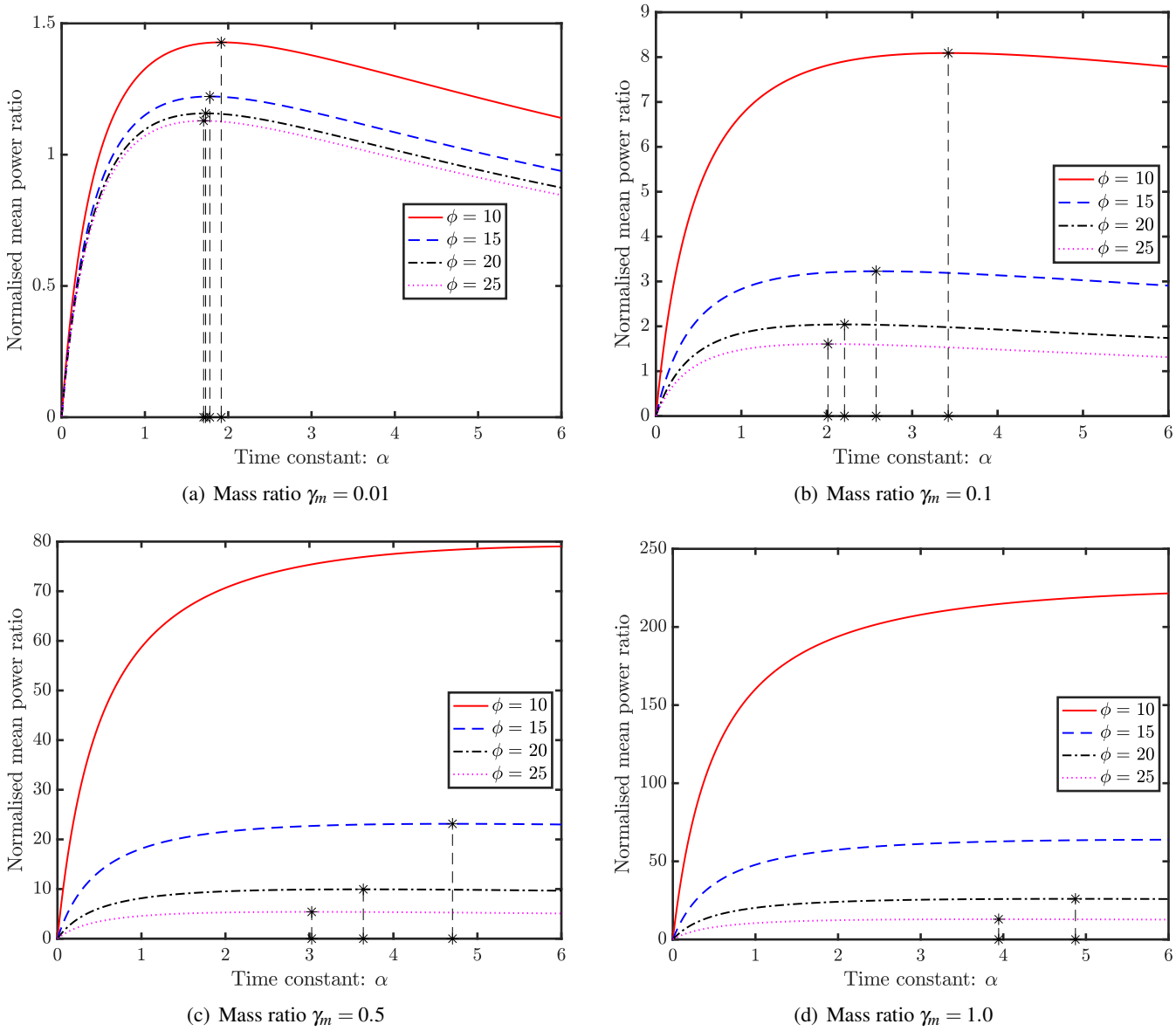

(a) Mass ratio $\gamma_m = 0.01$

(b) Mass ratio $\gamma_m = 0.1$

(c) Mass ratio $\gamma_m = 0.5$

(d) Mass ratio $\gamma_m = 1.0$

Figure 21. The normalised mean power ratio of a harvester without an inductor as a function of α for $\zeta = 0.1$, $\gamma_k = 0.5$ and $\kappa = 0.6$. The optimal values of β are obtained from (115). The * corresponds to the optimal value of $\alpha = 2.31$ for the maximum mean harvested power.

values of α given by equation (119). The amplification in the harvested power reduce for smaller values of the mass ratio and larger values of the inertial amplifier angle. When the mass ratio $\gamma_m = 1$ and the inertial amplifier angle $\phi = 10^\circ$, the mean power harvested form the proposed inertial amplifier based energy harvester can be over 200 times more than the power harvested form the classical energy harvester as can be observed in Figure 18(d).

5 Summary

This document developed the mathematical framework for the analysis of vibration energy harvesters incorporating inertial amplifiers. A cantilever beam with piezoelectric layers and tip mass subjected to base excitation is employed. The base excitation is considered to be both harmonic excitation and broadband random excitation. A reduced single-

degree-of-freedom electromechanical model with inertial amplifiers is employed in the analytical formulations.

The electromechanical coupling in the model is considered to be arising from a bimorph piezoelectric configuration. Two cases of energy harvesting circuits, namely, one with an inductor and another without an inductor, have been used. For both the cases, the governing equations are in general represented by coupled second-order ordinary differential equations and they are expressed in terms of non-dimensional coefficients. Additionally, the displacement and voltage response is also transformed into non-dimensional forms for clarity and simplicity. The voltage response of the system has been studied under deterministic harmonic excitation and optimal frequency for the maximum power generation has been obtained analytically. The randomness in the base excitation is modelled using a broadband Gaussian random process. Closed-form formulae for the average normalised harvested power for the energy harvesters without and with an inductor have been derived.

The main aspects discussed here include:

1. *Frequency for the maximum power:* For the case of deterministic harmonic base excitation, the non-dimensional frequency for maximum harvested power has been derived for both types of circuits. The exact solution involves the solution of a cubic equation for the circuit without the inductor and a quartic equation for the circuit with the inductor. Closed-form approximate expressions for the frequency of maximum harvested power have been derived for both cases. The expressions explicitly capture the parameters which contribute towards the frequency of maximum harvested power. They give physical insights and clearly demonstrate that power can be harvested at a lower frequency compared to the classical harvester.

2. *Optimal parameters for harmonic excitations:* The closed-form expressions for the non-dimensional frequency of maximum harvested power has been used to obtain the optimal parameter values of the inertial amplifier to maximise the power. Optimal values for stiffness, mass or the inertial amplifier angle can be obtained using the expressions provided. The optimal values involve the solution of a quadratic equation for the circuit without the inductor and a cubic equation for the circuit with the inductor.

3. *New closed-form power expressions:* Exact closed-form expressions for average normalised harvested power for energy harvesters without and with an inductor have been derived using contour integration techniques. These formulae provide physical insights and enable the derivation of optimal parameter sets to maximise harvested power even when the ambient bases excitation is not a harmonic excitation.

4. *Optimal parameters for random excitations:* Optimal parameters which maximise the harvested power belong to two groups, namely the parameters related to the electrical circuits and the parameters related to the inertial amplifier. They are interrelated. Explicit closed-form formulae have been derived which define their relationship to achieve maximum harvested power due to random excitations.

Results obtained from the derived average power equations have been illustrated numerically for selected parameter values. The limited analysis shown here highlights the fact that the average harvested power can be maximised for optimal parameters of the inertial amplifier. An optimally designed piezoelectric energy harvester with inertial amplifiers can deliver higher harvested power at a lower frequency.

References

1. Erturk, A. & Inman, D. J. *Piezoelectric Energy Harvesting: Modelling and Application* (Wiley-Blackwell, Sussex, UK, 2011).

2. Banks, H. T. & Inman, D. J. On damping mechanisms in beams. *Transactions ASME, J. Appl. Mech.* **58**, 716–723 (1991).

3. Blevins, R. D. *Formulas for Natural Frequency and Mode Shape* (Krieger Publishing Company, Malabar, FL, USA, 1984).

4. Adhikari, S. & Chowdhury, R. The calibration of carbon nanotube based bio-nano sensors. *J. Appl. Phys.* **107**, 124322:1–8 (2010).

5. Meirovitch, L. *Principles and Techniques of Vibrations* (Prentice-Hall International, Inc., New Jersey, 1997).

6. Adhikari, S., Bhattacharya, B. & Rastogi, A. Piezoelectric vortex induced vibration energy harvesting in a random flow field. *Smart Mater. Struct.* (2020). In press.

7. duToit, N. E. & Wardle, B. L. Experimental verification of models for microfabricated piezoelectric vibration energy harvesters. *AIAA J.* **45**, 1126–1137 (2007).

8. Adhikari, S., Friswell, M. I. & Inman, D. J. Piezoelectric energy harvesting from broadband random vibrations. *Smart Mater. & Struct.* **18**, 115005:1–7 (2009).

9. Ali, S. F., Friswell, M. I. & Adhikari, S. Piezoelectric energy harvesting with parametric uncertainty. *Smart Mater. & Struct.* **19**, 105010:1–9 (2010).

10. Renno, J. M., Daqaq, M. F. & Inman, D. J. On the optimal energy harvesting from a vibration source. *J. Sound Vib.* **320**, 386–405, DOI: 10.1016/j.jsv.2008.07.029 (2009).

11. Lin, Y. K. *Probabilistic Thoery of Strcutural Dynamics* (McGraw-Hill Inc, Ny, USA, 1967).

12. Nigam, N. C. *Introduction to Random Vibration* (The MIT Press, Cambridge, Massachusetts, 1983).

13. Bolotin, V. V. *Random vibration of elastic systems* (Martinus and Nijhoff Publishers, The Hague, 1984).

14. Roberts, J. B. & Spanos, P. D. *Random Vibration and Statistical Linearization* (John Wiley and Sons Ltd, Chichester, England, 1990).

15. Newland, D. E. *Mechanical Vibration Analysis and Computation* (Longman, Harlow and John Wiley, New York, 1989).